THESIS FOR THE DEGREE OF LICENTIATE OF ENGINEERING

Development of Novel *In Situ* ESEM Techniques for the Study of Water Interaction with Soft Materials

ANNA JANSSON

Department of Applied Physics

CHALMERS UNIVERSITY OF TECHNOLOGY

Gothenburg, Sweden 2013

Development of Novel *In Situ* ESEM Techniques for the Study of Water Interaction with Soft Materials

ANNA JANSSON

Department of Applied Physics
Chalmers University of Technology
SE-412 96 Gothenburg
Sweden
Telephone: +46 (0)31 772 10 00

The figure on the cover shows ESEM images of an individual cellulose fibre in contact with a water droplet (left) and an individual yeast cell in contact with an AFM probe (right) in the ESEM.

Printed by:
Chalmers Reproservice
Gothenburg, Sweden 2013

Development of Novel *In Situ* ESEM Techniques for the Study of Water Interaction with Soft Materials

ANNA JANSSON
Department of Applied Physics
Chalmers University of Technology

ABSTRACT

The transport of water is central to many applications of soft biomaterials; for example water management in personal care products, controlled drug release in pharmaceuticals and, on a fundamental level, the activities of living cells. Water transport through a material may occur in both liquid and gas phase, and is highly dependent on the microstructure. Understanding the relationship between structure and transport properties is the basis for predictive models and may aid the design of new functional materials. The environmental scanning electron microscope (ESEM) is a powerful tool when it comes to visualising the effects of hydration or dehydration of a specimen, facilitating the connection between microstructure and properties. However, there are still limitations when it comes to studying the transport of water through materials.

The aim of this work was to develop new ESEM-based methods that enable the *in situ* study of water transport in a controlled manner. A new experimental platform was created based on the combination of a nanomanipulator and a solution for local cooling of a surface in the sample chamber of the ESEM. Two different applications were chosen to test and evaluate the new technique, and to demonstrate its possibilities. The first application was the *in situ* controlled wetting of individual cellulose fibres. The goal was to capture the interaction between a fibre and water through simultaneous manipulation and imaging. A cellulose fibre was brought in contact with a water droplet situated on the cooled surface in the ESEM using the nanomanipulator. For the first time, the transport of liquid water by an individual cellulose fibre was imaged. Repeated experiments with different fibres showed a marked variation in absorptive capacity. The second application was the study of the osmotic response of individual yeast cells, which is intimately connected with water transport across the cell membrane. The nanomanipulator was coupled with a piezoresistive AFM sensor to enable the measurement of forces with high accuracy and a temporal resolution in the millisecond range. The relative humidity around the cells was rapidly increased. This resulted in cell expansion, analogous to a hyposmotic shock. The expansion could be followed in real time and cell size changes in the nanometre range were recorded using the AFM sensor. This method is highly interesting as a tool for single cell characterisation with focus on cellular water transport.

The results demonstrate the possibilities of the developed technique, but the flexibility of the setup allows the approach to be extended to other materials where the interaction with water and other fluids is of interest. Our work has advanced the field of *in situ* ESEM by enabling more controlled experiments with respect to liquid water absorption and transport as well as water vapour sorption and swelling.

Keywords: environmental scanning electron microscopy, in situ, manipulator, water interaction, water transport, swelling, cellulose fibre, yeast cell, osmotic shock

PREFACE

The research presented in this thesis was carried out at the Division of Microscopy and Microanalysis and in the Eva Olsson group at the Department of Applied Physics, Chalmers University of Technology, Gothenburg, Sweden, during the periods of March 2009 through February 2011 and January 2012 through April 2013, under the supervision of Prof. Eva Olsson and assistant supervisors Dr. Stefan Gustafsson and Prof. Anne-Marie Hermansson.

The following papers are included in this thesis:

Paper I. **Novel Method for Controlled Wetting of Materials in the Environmental Scanning Electron Microscope**
A. Jansson, A. Nafari, A. Sanz-Velasco, K. Svensson, S. Gustafsson, A.-M. Hermansson, and E. Olsson

Microscopy and Microanalysis 2013, 19(1), 30-37

Paper II. **Monitoring the osmotic shock response of single yeast cells through force measurement in the ESEM**
A. Jansson, A. Nafari, K. Hedfalk, E. Olsson, K. Svensson and A. Sanz-Velasco

To be submitted

My contribution to the appended papers:

Paper I: I co-developed the experimental setup, did all the experimental work, carried out the evaluation in discussion with my co-authors and wrote the paper.

Paper II: I co-developed the experimental setup, did the microscopy work and evaluation together with my co-authors, and was the main author of the paper.

Anna Jansson
Gothenburg, April 2013

ABBREVIATIONS

ESEM	Environmental scanning electron microscope
FSP	Fibre saturation point
RH	Relative humidity
SEM	Scanning electron microscope
SVP	Saturated vapour pressure
TEM	Transmission electron microscope

TABLE OF CONTENTS

1 INTRODUCTION

This chapter provides a background for the thesis and a motivation for the development of new *in situ* ESEM methods related to the study of the interaction between water and soft biomaterials. It introduces the specific systems used to test and evaluate the new techniques, and explains the importance of water transport in these systems. In relation to this, the aim and scope of the work are clarified.

1.1 Background

In our everyday lives, we are surrounded by materials that interact with water, and where this interaction is pivotal to the function of the material. For instance, in personal care products, we rely on the ability of the absorbent material to quickly absorb and transport liquids. Food substances are exposed to water during cooking as well as in the mouth and digestive system, and the release of drugs from pharmaceutical products depends on the interaction of the product formulation with the fluids in the body. On a very basic level, the living cells of our bodies need water in order to function. The interaction of different materials with water thus constitutes an important field of study.

The structures exemplified above can all be categorised as *soft biomaterials* in the wide sense of the term. Among the many definitions of a biomaterial, we find truly biological materials, biologically derived materials and man-made products designed to function in contact with a living system. In this thesis, the term *soft biomaterials* shall be used to signify supramolecular biomaterials, which typically have a complex build-up and often feature functional structures at a range of different length scales. Such materials usually exhibit a dynamic response to water exposure, where transient microstructural changes occur and the water transport properties evolve with time as a result. Furthermore, different transport mechanisms, i.e. diffusion or flow or a combination thereof, may dominate the behaviour at different length scales. In many applications, water transport is an aspect of particular importance, and increased knowledge of the relationship between materials structure and water transport properties could enable the design of new materials where the structure is tailor-made to yield specific transport properties.

A few decades ago, the advent of the environmental scanning electron microscope (ESEM) opened up unique possibilities of studying the interaction between materials and water at the micro- and nanometre scale. In contrast to the high vacuum requirement of a conventional scanning electron microscope (SEM), the ESEM is designed to operate in a gaseous environment at pressures up to 20 torr. The presence of a gas enables the imaging of electrically insulating specimens without the need for applying a conductive coating. If the gas is water vapour, additional possibilities arise. By regulating the specimen temperature and water vapour pressure inside the sample chamber of the ESEM, the relative humidity (RH) at the sample can be controlled. In practice, this means that

water-containing materials can be stabilised and viewed in their native state, omitting the need for preparatory steps that remove the water content and potentially cause artefacts in the form of structural changes. Moreover, increasing or decreasing the relative humidity may cause hydration or dehydration of the specimen, in the gaseous (below 100% RH) or liquid regime (above 100% RH). The technique has been extensively used to study different materials and phenomena, and a comprehensive review of the principles as well as some important applications is given in (Stokes, 2008).

The ESEM lends itself particularly well to *in situ* investigations, where dynamic processes can be followed in real time, and for this reason has been referred to as "a lab in a chamber" (Stokes, 2008). For example, the absence of conductive coatings on electrically insulating materials makes it possible to mechanically manipulate specimens without constraints imposed by a coating, see e.g. (Rizzieri, Baker, & Donald, 2003) and (Thiel & Donald, 1992). Moreover, the response to hydration and dehydration, which may involve effects such as swelling, dissolution or rearrangement of structures, can be examined, see e.g. (Dragnevski & Donald, 2008) and (Jenkins & Donald, 2000). However, when it comes to the study of the transport of water through materials, reported ESEM applications are scarce. This may, in part, be attributed to the limitations of the standard set-up for dynamic wetting experiments in the ESEM.

In situ wetting of a specimen in the ESEM is usually accomplished by increasing the relative humidity to induce condensation onto the specimen surface. This can be done by simply raising the water vapour pressure in the sample chamber of the ESEM or, equivalently, decreasing the temperature of the sample to get above the dew point (100% RH). For many applications involving liquid water transport, this traditional method does not offer sufficient control over the wetting process. Water condenses in the form of droplets or a continuous film on the specimen surface, depending on the nature of the material. Hence, the point of interaction between water and specimen is not well defined. Also, as the water is relatively opaque to the electrons used for imaging, it may obscure the underlying structures, as illustrated in Figure 1. Together, these aspects render this traditional method generally inappropriate for studies of water transport and related effects on the microstructure.

A better control of the point of interaction can be achieved by using a microinjector to locally dispense water onto the specimen surface. This has been done in several studies using water and other liquids, see e.g. (Camacho-Bragado, Dixon, & Colonna, 2011) and (Wei, Mather, Fotheringham, & Yang, 2002), but does not solve the problem of the water obscuring the sample structure. Reingruber and coworkers used an innovative approach to study the wetting and drying of membranes in the ESEM, allowing the study of the transport of water in the liquid and gas phases inside the membrane structure (Reingruber, Zankel, Mayrhofer, & Poelt, 2012). To our knowledge, no other methods for direct imaging of water transport in the ESEM are currently available. Hence, there is a need for new ESEM-based methods that offer greater control over the wetting process and thereby enable the *in situ* study of water transport.

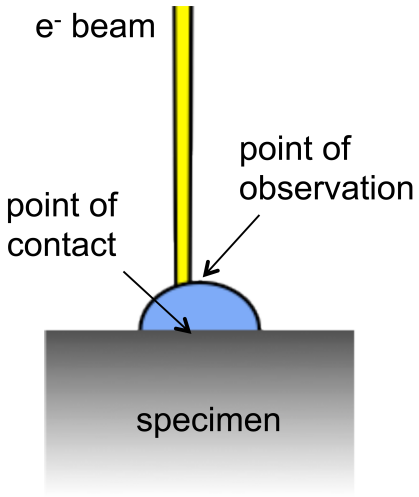

Figure 1. Schematic illustration of the problem of imaging a specimen with condensed water on its surface. The water is relatively opaque to the electrons in the incident electron beam and may therefore obscure the underlying structure of the specimen. Thus, the point of observation is not the same as the point of interaction between water and specimen.

Many soft biomaterials undergo swelling as water enters the material microstructure. This can apply to liquid water as well as water vapour. In the ESEM, the process of swelling can be followed through imaging as in e.g. (Jenkins & Donald, 2000) and (Montes-H, Geraud, Duplay, & Reuschle, 2005). However, the measurement of the extent and rate of swelling may be complicated by imaging-related aspects – especially for small structures that challenge the resolution of the microscope under given imaging conditions, or in the case of rapid events where the image frame rate is limited by the maximum tolerable scanning speed that can be used without compromising the image quality. Hence, techniques that enable accurate measurement of the swelling behaviour at a high temporal resolution might aid the characterisation of certain materials systems that are difficult to study using traditional ESEM methods.

This work concerns the development of new *in situ* ESEM methods to enable the study of water transport in soft biomaterials in a controlled manner. A flexible experimental platform of wide applicability to different materials is envisioned. The motivation stems from our collaboration with different partners whose work is focused on aspects of water transport.

Several partners are found in SuMo Biomaterials, a VINN Centre of Excellence that brings together industrial and academic scientists united by a common interest in understanding the mass transport properties of supramolecular biomaterials and developing predictive models as a basis for the design of new functional materials. Water is an essential ingredient of most research problems within SuMo. Therefore, there is a general interest in the development of new methods that can advance the knowledge of relationships between microstructure and water transport, especially with a focus on the dynamics of the interaction.

Through collaboration with the SuMo participant Södra Cell AB, cellulose fibres from pulp were used to test and evaluate the new *in situ* ESEM technique and illustrate its possibilities. Cellulose fibres and their wetting properties are at the heart of the pulp and paper industry, and much research is devoted to understanding the structural changes that occur in the cellulose fibre during drying and wetting processes (Laivins & Scallan, 1993). The fibres were chosen for their high capacity for water uptake and swelling, to give a clear indication of water absorption and transport during the *in situ* investigations.

The wetting properties of cellulose fibres in the ESEM have previously been addressed in a number of reports; see e.g. (Jenkins & Donald, 1997), (Karlsson, Andersson, Berntsson, Chihani, & Gatenholm, 1998), (Jenkins & Donald, 1999), (Jenkins & Donald, 2000), (Gellerstedt, Wågberg, & Gatenholm, 2000). However, these studies all employed the traditional approach of *in situ* hydration where the relative humidity is increased by raising the pressure or lowering the sample temperature. Moreover, few attempts have been made at isolating individual fibres. As water absorption in a fibre network is a complex process with contributions from the fibre properties as well as the network structure (Karlsson, Andersson, Berntsson, Chihani, & Gatenholm, 1998), studying a cellulose fibre in isolation is important and complements previous studies with the aim of understanding the transport mechanisms involved.

A second type of soft biomaterial structure was used to demonstrate additional aspects of the possibilities of the new technique. Widely different in character, it was inspired by our collaboration with Dr Kristina Hedfalk in the Department of Chemistry and Molecular Biology at the University of Gothenburg whose research is focused on the structure and function of membrane proteins in cells. Cells surround themselves with a membrane that is permeable to water. The permeability is increased by the presence of water channels called *aquaporins*. When exposed to a so-called *hyposmotic shock*, i.e. a decrease in the concentration of solutes of the external medium, cell swelling is induced. As all cells are highly dependent on the ability to maintain a constant volume, they have mechanisms to regulate their volume in response to perturbations. The role of water channels in the cell swelling and volume regulation is not known in detail (Pasantes-Morales & Cruz-Rangel, 2010), although gating mechanisms regulating the activity of water channels in yeast cells have been suggested as protective measures against the effects of osmotic shocks (Fischer, et al., 2009) (Soveral, Madeira, Loureiro-Dias, & Moura, 2008). Understanding the structure, function and gating of aquaporins is important as a foundation for the development of drugs directed toward the water transport activity of cells (Öberg & Hedfalk, 2012).

Yeast cells have been extensively used as models to study the processes involved in the response to osmotic shock, see e.g (Soveral, Madeira, Loureiro-Dias, & Moura, 2008) and (Klipp, 2005). Results on yeast may elucidate mechanisms relevant to human cell physiology, because the adaptive strategies employed by the cells are highly conserved through evolution (Somero & Yancey, 1997). Moreover, it is possible to produce human aquaporins in yeast cells and to design cell strains expressing varying amounts of aquaporins (Öberg & Hedfalk,

2012) (Fischer, et al., 2009), enabling the study of aquaporin function in a controlled manner. A common way to study the yeast response to osmotic shock is to mix a suspension of cells with a solution of different osmolality than the cell interior. The response can then be followed by stopped-flow technique, see e.g. (Fischer, et al., 2009) and (Soveral, Madeira, Loureiro-Dias, & Moura, 2008). However, as this provides an ensemble average of the cell response, complementary techniques for single cell characterisation are desired. There are ways to study the single cell response, e.g. by optical microscopy (Soveral, Madeira, Loureiro-Dias, & Moura, 2008), but the accuracy of volume determination and the temporal resolution are limited. The development of methods enabling single cell monitoring of osmotic response at a high temporal resolution is therefore of value to the field. The humidity-controlled environment of the ESEM provides a suitable basis for such a method, under the assumption that a humidity increase creates a cell response similar to that induced by a hyposmotic shock in an aqueous environment.

1.2 Aim of the work

The aim of this work was to improve the control of *in situ* experiments in the ESEM towards the successful study of water interaction with, and transport in, soft biomaterials. To achieve this aim, one needs to overcome the limitations of traditional ESEM-based approaches to hydration and wetting, where water transport and the contact point between the water and the material have not been the focus. This has been done through the development of new methods. Our goal with the method development was to create a flexible platform of wide applicability to different materials. In order to test and evaluate the technique, and at the same time demonstrate its possibilities, it was applied to two different materials with very different types of water interaction.

The first application was the *in situ* controlled wetting of individual cellulose fibres. Here, the objective was to study the interaction between a fibre and a water droplet in the ESEM, and more specifically to visualise the swelling and the effects of water transport.

In the second application, the objective was to prove the concept of a technique that could measure the osmotic response of single yeast cells in the ESEM in the form of volume change. The focus was on the dynamics of the process, to show that we could follow the time dependent expansion of a single yeast cell with a sufficient temporal resolution.

A further aim of this thesis is to convey the wide range of applications and flexibility of the developed techniques to the study of interaction, swelling and liquid water transport in different materials.

2 WATER TRANSPORT

The transport of water is a common denominator for the work of this thesis. This chapter provides a literature review on water transport for cellulose fibres as well as for yeast cells, to increase the understanding and aid the interpretation of the results of the *in situ* ESEM experiments.

2.1 Cellulose fibres

The interaction between water and cellulose fibres is important in many materials-related applications, e.g. in the papermaking (Perkins & Batchelor, 2012) and wood product industries (Bergman, et al., 2010). To facilitate the understanding of the mechanisms involved in the water uptake and transport, this section features a brief introduction to the structure of the cellulose fibre. Here, we are concerned with cellulose fibres originating in wood. The description is limited to the cellulose fibre itself and hence does not include the organisation of fibres and other structures in wood. Furthermore, as the fibres used in the *in situ* ESEM investigation are pulp fibres from softwood (coniferous trees), the discussion shall only concern the structure and properties specific to softwood fibres.

2.1.1 Structure

Softwoods consist of two different types of cells, where the largest group (90-95%) are the so-called *tracheids*. These are typically 2-4 mm long and 20-40 μm thick (Sjöström, 1993), but narrower toward the ends. The tracheids are the cellulose fibres typically used in the pulp and paper industry (Theliander, Paulsson, & Brelid, 2002), and also in the present work.

In the wood, the tracheids are longitudinally oriented, i.e. along the direction of the stem or branches. They are dead cells, whose key functions are to provide mechanical support and to conduct water up the stem of the tree (Rowell, 2012). These different purposes are reflected in the structure of the fibre, as it consists of a cell wall with a hollow cavity, the *lumen*, running along the centre. The lumen plays an important role for the water transport through the fibre. In the wood produced during spring (*earlywood*), when the tree grows fast and requires an efficient water transportation system, the lumen is wide and the cell wall thin. Conversely, in the slow growing, denser *latewood* produced during summer, the fibres develop a thick cell wall with a narrower lumen (Sjöström, 1993) (Theliander, Paulsson, & Brelid, 2002) (Rowell, 2012).

A schematic drawing of the structure of the cell wall is shown in Figure 2. It consists mainly of cellulose, hemicelluloses and lignin, and has a highly organised, hierarchical structure. Some aspects of the ultrastructure of the cell wall are still being debated and the terminology of different elements is not unified. A simplified description is given here. Cellulose molecules are arranged into bundles called *elementary fibrils* that are a few nanometres wide. These are arranged into *microfibrils* (10-20 nm wide), which are arranged into greater

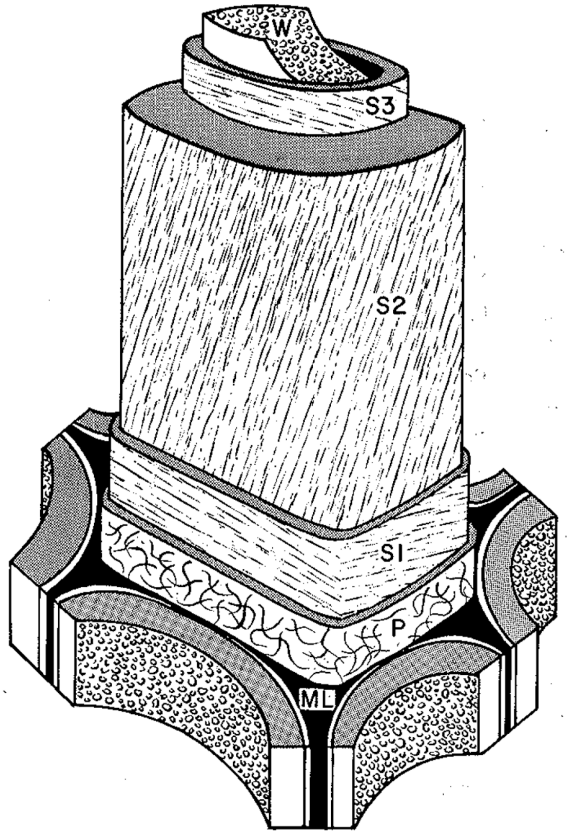

Figure 2. Schematic drawing of the cell wall layers. S1, S2 and S3 are the three lamellae of the secondary wall. P is the primary wall and ML the middle lamella. W is the so called *warty layer* lining the lumen. From (Côté, 1967), reprinted by permission of the University of Washington Press.

fibrils and lamellae that build up the cell wall layers known as the primary wall and the secondary wall. In the primary wall, the microfibrils are disordered but in the thicker secondary wall, they form three anisotropic lamellae where the angle of fibril arrangement varies between the layers. Between adjacent cells, there is the so-called *middle lamella* that consists mostly of lignin and holds the cells together. The warty layer is a thin, amorphous layer lining the lumen. Throughout the fibrillar structure of the cell wall, lignin and hemicelluloses are present as encrusting materials (Theliander, Paulsson, & Brelid, 2002) (Sjöström, 1993).

2.1.2 Water-fibre interaction

As explained in section 2.1.1, the cellulose fibre has mainly two domains – the cell wall and the central cavity, or lumen. Both interact strongly with water, but through different mechanisms. This section provides a brief overview of the interaction between water and different parts of the cellulose fibre.

The cell wall is a hygroscopic material, i.e. it has an affinity for water, due to the hydroxyl groups present on the cellulose as well as hemicellulose molecules. As a consequence, the fibre will absorb moisture from the air and the moisture content will come to equilibrium with the environment according to the relative humidity and temperature of the air (Bergman, et al., 2010). The cell wall is also a

porous structure at the nanometre level, and the void volume in the cell wall increases dramatically during Kraft pulping as the wood is delignified to separate the fibres. Hence, pulp fibres have a much higher porosity than native fibres (Andreasson, Forsström, & Wågberg, 2003). The pore volume in the cell wall has a large influence on the swelling properties as the fibre when exposed to water (Östlund, Köhnke, Nordstierna, & Nydén, 2009).

Furthermore, the lumen is essential for the water transport properties of the fibre (Sjöström, 1993). When the fibre is exposed to liquid water, capillary forces draw water up the lumen due to a combination of the water-cellulose interaction and the water-air surface tension (Bergman, et al., 2010).

Water in the cellulose fibre has been classified in different ways in the literature. A commonly used description, although somewhat simplified, is "bound" and "free" water. The water in the cell wall is bound, held by intermolecular attractive forces, while the water in the lumen is considered free, i.e. not bound in any way except by capillary forces. The so-called *fibre saturation point* (FSP) is the moisture content at which the fibre wall is saturated with water but no water exists in the lumen. This is generally around 30wt% (Bergman, et al., 2010), but can vary between 20wt% and 50wt% depending on tree species (Rowell, 2012). Below the FSP, the moisture content depends on the relative humidity and temperature of the surrounding air. The moisture content of the cellulose fibre can only exceed the FSP if the fibre is exposed to liquid water. All water absorbed beyond the FSP is "free water" contained in the lumen, not bound in any way except by capillary forces. In wood, moreover, dimensional changes with respect to moisture content, such as swelling or shrinking, only occur below the FSP (Bergman, et al., 2010) (Rowell, 2012).

When a fibre absorbs liquid water, its moisture content can increase at a faster rate than possible by water vapour sorption, and the rate of absorption is highest in the longitudinal direction, i.e. in the direction of the lumen. The rate also depends on how quickly the air in the lumen can escape and be replaced by water. The fibre can absorb liquid water until its maximum moisture content is reached. The maximum moisture content can be over 200wt% (Bergman, et al., 2010).

Another important aspect of the water-fibre interaction is the process called *hornification*. It refers to changes in the properties and structure of cellulose fibres in wood pulps or paper upon drying or removal of water. The pore volume in the cell wall collapses and the polymer structure stiffens. These changes are described as irreversible or partially reversible (Fernandes Diniz, Gil, & Castro, 2004), and they are manifested in several different macroscopic properties of the pulp or paper. For example, the water uptake and swelling upon rewetting is diminished, and paper products suffer a loss in tensile strength. Hornification is thus an area of interest particularly in the pulp and paper industry (Östlund, Köhnke, Nordstierna, & Nydén, 2009), and much research is devoted to understanding the underlying mechanisms in order to be able to control the phenomenon. The subject is still under debate, and some theories that have been put forward describe the effect as an increase in the degree of crosslinking

within the fibre wall due to interfibrillar hydrogen bonding or, alternatively, lactone bridge formation (Fernandes Diniz, Gil, & Castro, 2004). The hornification increases with the number of cycles of drying and rewetting. In addition, a low lignin and hemicellulose content has been shown to amplify the effects of hornification (Laivins & Scallan, 1993).

2.2 Yeast cells

Paper II focuses on the development of a method for studying osmotic response in yeast cells in the ESEM. At the heart of this problem lies the water transport properties of yeast cells and how they affect the response to changing osmotic conditions in the environment of the cell. Changes in osmolality that perturb the cell volume are often referred to as *osmotic shocks*, and the process of active volume regulation is called *osmoregulation*. The complex details of the cell physiology and the mechanisms of osmoregulation are far outside the scope of this thesis. However, a basic level of knowledge concerning the yeast cell structure and the adaptive strategies of the cell is helpful for the understanding of the purpose of the method development. Therefore, this section gives a brief introduction to the concepts involved.

2.2.1 Response to osmotic shock

All cells are highly dependent on the ability to maintain a constant volume (*homeostasis*), and therefore have mechanisms to regulate their volume in response to perturbations. The cell volume is governed by the amount of water in the interior of the cell, and even small changes in water content may adversely affect important process related to cell signalling and communication as well as the integrity of functional molecules (Pasantes-Morales & Cruz-Rangel, 2010). As the cell membrane is permeable to water, a net water flux into or out of the cell results in expansion or shrinkage, respectively. The flow of water across the cell membrane follows the rules of osmosis, where the relationship between the extracellular and intracellular concentrations of solutes (*osmolytes*), or *osmolality,* determines the direction of water flow (Verbalis, 2010).

A *hyposmotic shock* is induced if the external osmolality drops rapidly. The immediate effect is a passive response of the cell in the form of swelling due to water influx. After some time, however, an active regulatory process sets in to bring the cell volume back toward normal. This process involves the export of solutes from the cell to even out the osmotic gradient and reverse the water flux (Verbalis, 2010)(Tamás, et al., 2003). The active response, or osmoregulation, occurs more slowly than the passive response (Marechal, Martinez de Marafion, Molin, & Gervais, 1995) (Verbalis, 2010).

Cell volume changes occur continuously under "normal" physiological conditions in response to different processes. However, pathological states of various kinds may cause more serious imbalance in osmolality. One place where the consequences of cell volume perturbation are particularly dramatic is in the brain. The skull is a rigid construction that restricts the brain volume and the ability of the tissue to expand is thus limited. Therefore, brain edema, which may result from a number of different conditions including head trauma (Pasantes-

Morales & Cruz-Rangel, 2010), is a serious state that can lead to neurological damage or death (Verbalis, 2010).

2.2.2 Aquaporins

Aquaporins are membrane proteins that function as channels for water and certain solutes. They are crucial for the regulation of cell volume, and severe disorders and diseases can arise if their function is compromised. Therefore, the study of aquaporin structure, function and regulation is important as a step toward developing future drugs that target the water transport activity of cells. The aquaporins are divided into two categories: *orthodox aquaporins* and *aquaglyceroporins*, where the former type acts as channels mainly for water while the latter transport water and glycerol. 13 different aquaporins have been identified in humans (Öberg & Hedfalk, 2012). In the brain, the aquaporin AQP4 is of particular importance for the water permeability, and studies indicate that its activity affects both the extent of cellular swelling under hyposmotic conditions and the volume regulatory response. Mechanisms for the regulation of AQP4 activity have been proposed. However, the current lack of inhibitors for this membrane protein makes it difficult to study the role of AQP4 in a direct way (Pasantes-Morales & Cruz-Rangel, 2010). Identifying substances that could work as AQP4 inhibitors is thus an important task and one of the overall goals of the study of aquaporins.

To enable the characterisation of membrane proteins and their functions, one challenge is to ensure availability of the proteins in sufficient amounts. Techniques have been developed for overproducing proteins in the membranes of host organisms, e.g. yeast cells (Öberg & Hedfalk, 2012). Yeast cells are often used as models in the study of osmotic response, see e.g. (Soveral, Madeira, Loureiro-Dias, & Moura, 2008) and (Klipp, 2005). There are many species of yeast, and the most studied is *Saccharomyces cerevisiae* or "baker's yeast". However, there is another species of interest in this context, namely *Pichia pastoris*, which has proven a successful host for the overproduction of the human aquaporins (Öberg & Hedfalk, 2012). It is also possible to engineer the expression of native proteins in a strain of cells. For example, by deleting the gene that encodes a certain membrane protein in one strain and inducing overproduction in another strain, the function of the protein can be examined through the response to external stimulus. For *P. pastoris*, this approach was used by Fischer and co-workers to study the water transport activity of the orthodox aquaporin Aqy1, which is the only aquaporin native to *P. pastoris* (Fischer, et al., 2009).

Fischer and co-workers hypothesise that Aqy1 is sensitive to mechanical stimulus in the form of membrane tension and curvature, and that this may be a mechanism of regulation or "gating" of the water channel that protects the cell from the effects of an osmotic shock (Fischer, et al., 2009). A similar suggestion was made by Soveral and co-workers, who studied *S. cerevisiae* yeast cells. This species expresses two aquaglyceroporins and two orthodox aquaporins, including Aqy1 (Fischer, et al., 2009). They believe that Aqy1 is inhibited under hyposmotic shock due to development of membrane tension upon rapid cell swelling. They further speculate that this mechanism could be a first tool of the

cell to decrease the water influx across the cell membrane while the mechanism for exporting solutes is being triggered, as the water channel inhibition can be expected to give a more rapid response (Soveral, Madeira, Loureiro-Dias, & Moura, 2008).

3 EXPERIMENTAL

This chapter collects information on the experimental aspects of the work. It introduces the working principles of the environmental scanning electron microscope (ESEM), based on the comprehensive review by (Stokes, 2008). It also describes the investigated materials in more detail, i.e. cellulose fibres and yeast cells, along with the sample preparation for the *in situ* ESEM experiments. The information provided here serves as a platform for the following chapter 4, which concerns the development of new methods for *in situ* studies of water transport in the ESEM.

3.1 Environmental Scanning Electron Microscopy

Environmental scanning electron microscopy is a technique used to investigate the microstructure of materials in a controlled sample environment. It was developed during the 1970s and 80s as a response to the limitations of conventional scanning electron microscopy (SEM) with respect to sample requirements and flexibility of experiments. In a conventional SEM, high vacuum is maintained throughout the electron-optics column and the sample chamber, in order to prevent excessive scattering of the primary electron beam. To comply with the high vacuum requirement, the specimen has to fulfil certain conditions. Firstly, it must not contain any volatile substances, such as e.g. water or oil. Secondly, specimens need to be electrically conductive or they will accumulate negative charge during imaging with electrons, resulting in adverse effects on the image quality. These constraints affect the possibilities of examining certain types of materials with SEM, e.g. many biological materials and food substances as well as most polymers (Stokes, 2008).

There are ways to circumvent these limitations; volatile substances can be removed using one of many sample preparation techniques (e.g. freeze-drying or chemical fixing) and electrically insulating materials can be coated with a conductive layer to reduce charging. However, these types of sample preparation may change the structure of the material, obscure fine details or introduce other artefacts, possibly leading to misinterpretation of images. Moreover, applying a coating might reduce the chances of obtaining intrinsic contrast that can yield information about different regions of the sample. It may also limit the possibilities of performing dynamic experiments *in situ* (Stokes, 2008).

The environmental scanning electron microscope (ESEM) [1] bypasses the problems mentioned above and hence offers greater freedom in the choice of specimen and the design of experiments. The essential difference between a conventional SEM and an ESEM is the ability of the latter to operate with a relatively small amount of gas in the sample chamber. To be able to function at non-vacuum conditions, the microscope is equipped with a series of pressure-limiting apertures and a differential pumping system that limits the amount of

[1] The term ESEM is a trademark of FEI Company (originally Electroscan). Here, however, it is used as a general term that refers to all SEMs with the ability to operate under elevated pressures.

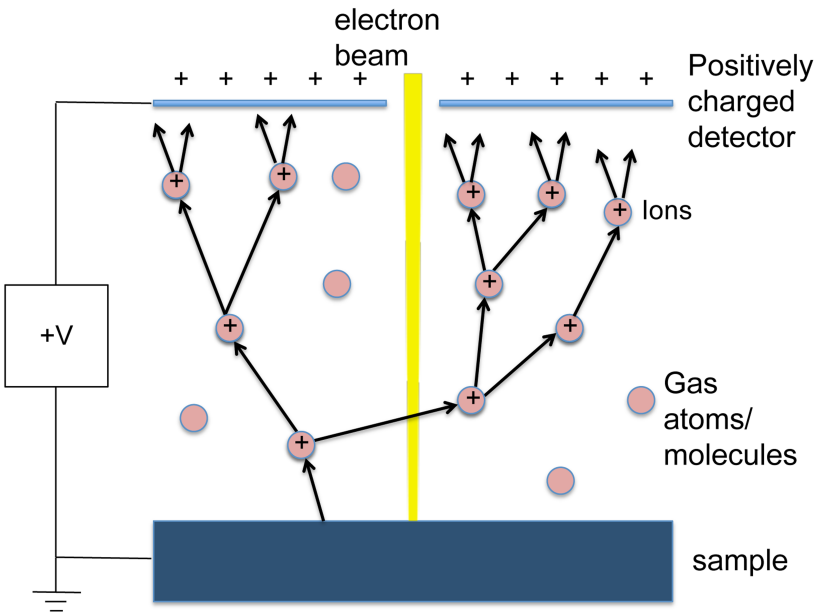

Figure 3. Schematic representation of the signal detection and charge compensation principle in the ESEM. Electron trajectories are illustrated by arrows. An electron leaving the sample surface is accelerated toward the positively charged detector, and collisions with gas atoms/molecules creates a cascade of electrons that amplify the signal. The positive ions resulting from the collisions drift toward the sample surface where they recombine with electrons on the surface.

gas in the electron-optics column and keeps the upper section, where the electron source resides, at high vacuum (Stokes, 2008).

Due to the presence of a gas, the principle of signal detection differs from that of a conventional SEM. The detector acts as the final pressure-limiting aperture and has a strong positive bias that attracts the electrons emitted by the specimen. The imaging gas plays an active role by enabling signal amplification through ionising collisions with the gas atoms/molecules. The resulting cascade of electrons are accelerated toward the detector, and the positive ions left in the gas are attracted towards the specimen surface where they recombine with free electrons to prevent the build up of static charge in the material. This process, illustrated in Figure 3, makes it possible to image insulating specimens without applying a conductive coating (Stokes, 2008).

There are a number of different gases that can be useful in the ESEM, and the choice depends on the material under study as well as the purpose of the investigation. Water vapour constitutes a special case where, in addition to signal amplification, the gas can also be used to stabilise water-containing specimens or even perform dynamic experiments involving the wetting or drying of materials *in situ*.

To control the state of hydration of a sample, both its temperature and the water vapour pressure in the surrounding environment must be considered since these are the factors determining the relative humidity at the sample site. The saturated vapour pressure (SVP) curve, depicted in Figure 4, is part of the phase

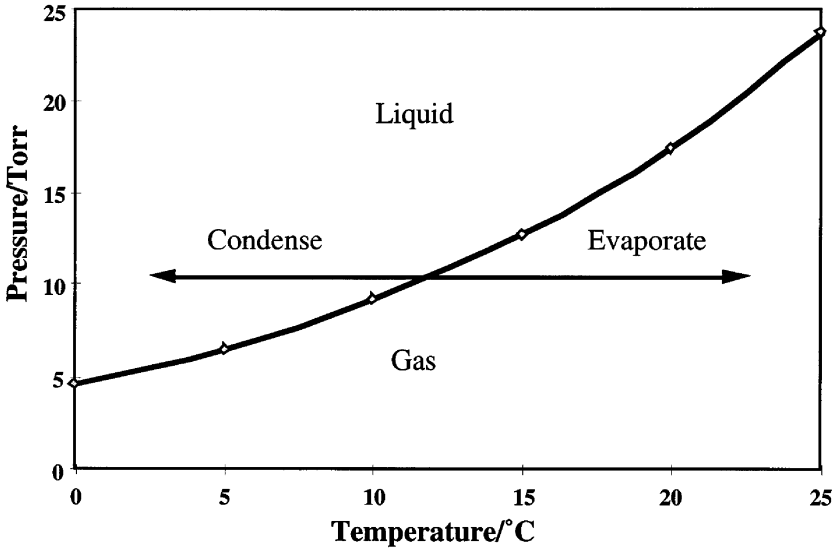

Figure 4. The saturated vapour pressure curve for water. Reprinted from (Donald, He, Royall, Sferrazza, Stelmashenko, & Thiel, 2000) with permission.

diagram for water and maps out different points of thermodynamic equilibrium between the liquid and gaseous phases. It helps us determine the combination of pressure and temperature needed to balance evaporation from and condensation onto the specimen in order to stabilise its moisture content in the microscope chamber. However, since many hydrated specimens contain aqueous phases with dissolved solutes such as e.g. salts and different biomacromolecules, the curve needs to be downshifted to take into account the water activity of the sample. If an aqueous phase of a specimen has water activity a_w, the equilibrium vapour pressure p_{eq} can be related to the SVP of pure water p_0 at the same temperature by

$$p_{eq} = a_w p_0$$

and the relative humidity can be expressed as $RH = a_w \cdot 100$.

If we enter the non-equilibrium regimes above or below the SVP curve in the phase diagram, condensation or evaporation will occur. This may be utilised to hydrate or dehydrate the specimen *in situ*, while the dynamics of the process are being followed in real time through imaging with the electron beam. Thus, certain properties of the material under study can be directly related to its microstructure.

Before microscopy can begin, the pressure inside the sample chamber must be brought down to operating pressures and the air must be replaced with water vapour. For moist specimens sensitive to dehydration, this is an important step. Purge-flood cycles can be employed to successively exchange air for water vapour. To boost the water vapour pressure around the specimen, a few droplets of water can be placed at a non-cooled area close to the specimen. These will evaporate at an early stage during pump-down (Stokes, 2008).

The microscope used throughout our experimental work was an FEI Quanta 200 FEG ESEM (FEI Company, Hillsboro, OR, USA). Additional equipment consisted of a Peltier cooling stage capable of operating in a temperature range of -25°C to 55°C, as well as the *in situ* sample stage developed in this work and its electronic control equipment. For details concerning imaging parameters and environmental conditions, see sections 4.2 and 4.3.1.

3.2 Materials and sample preparation

Two different types of material were used within the frame of this work – cellulose fibres in the controlled wetting experiments in paper I and yeast cells in the osmotic response studies of paper II.

3.2.1 Cellulose fibres

The cellulose fibres used in the investigations originated from softwood kraft pulp provided by Södra Cell AB (Värö, Sweden). Two types of samples were used, differing in the way the fibres had been prepared. One of the batches had been mercerised, i.e. treated with sodium hydroxide (NaOH), reducing the hemicellulose content to approximately 9% by weight. The other batch remained untreated, and thus contained a higher fraction of hemicellulose. Both batches were "never-dried" when obtained from the supplier, and they were stored in a refrigerator (below 8°C) to prevent drying and hornification prior to sample preparation.

To prepare a specimen for microscopy, a single fibre was extracted from pulp using a pair of tweezers and glued to an aluminium (Al) wire with a diameter of 0.3 mm using epoxy resin. Scissors were used to cut the tip of the fibre; this was done to expose the lumen and make it accessible for water transport in preparation for the wetting experiment. The resin was allowed to dry in air, during which time the fibre was exposed to dehydrating conditions. Hence, it should be pointed out that at the time of insertion into the microscope, the specimen was no longer moist.

Despite the fact that all fibres in a batch of pulp undergo the same treatment during the pulping process, there is typically a large variation in structure and properties among the different individual fibres. This is important to point out since it has a bearing on the experimental results when it comes to water absorption and transport. There are several different properties that can vary from fibre to fibre. One important factor is what part of the tree stem the fibre originates from. The position in the radial direction of the stem determines the growth period during which the fibre was formed. This, in turn, is strongly related to its structure and function. As mentioned in section 2.1.1, *earlywood* is optimised for water transport while *latewood* is optimised for mechanical strength. At the fibre level, this means that earlywood fibres have a thinner cell wall and a larger lumen than latewood. The fibre morphology also varies as a function of genetic factors. Hence there can be considerable variations between different individuals of a tree species as well as different parts of a stem – even within a single growth ring (Sjöström, 1993).

The pulps used for our investigations contained material from several different trees and from different parts of the stem. In light of the information above, one could therefore expect to see some variation in the appearance of different fibres and in their response to water exposure.

3.2.2 Yeast cells

The yeast cells used in the measurements were *Pichia pastoris* wild type, obtained from Kristina Hedfalk at the University of Gothenburg (Gothenburg, Sweden) in the form of a suspension. The suspension had been prepared from a liquid cell culture where the yeast cells were grown in YPD (Yeast extract Peptone Dextrose). The rationale for choosing a liquid cell culture over an agar plate culture was based on the importance of a uniform cell population with respect to age and growth conditions for the sake of reproducibility of the experimental results.

For the *in situ* ESEM experiments, the cell concentration of the suspension should be such that an appropriate amount of cells attach to the substrate. If the concentration would be too high, cells would attach in clumps; if too low, very few or no cells would attach. To solve this problem, the optical density (OD) of the suspension was used as a guide. Since previous examinations had shown that a suspension of optical density OD_{600}=2 resulted in an appropriate density of cells attached to the sample holder upon preparation, the liquid cell culture was resuspended to OD_{600}=2.

To ensure fresh samples, the experiments were performed within 24 hours of the preparation of the cell suspension. An aluminium wire with a diameter of 0.3 mm was used as a substrate for the cells. The wire was inserted into a slot in the Cu cylinder (which will be described in more detail in chapter 4), fastened with a screw and then bent to the side to become almost parallel to the vertical Cu wall (see Figure 5). This was done to increase the accessibility of the Al surface to the cantilever tip of the force sensor used in the *in situ* measurements. The wire was then immersed in the sample suspension for approximately 30-60 s.

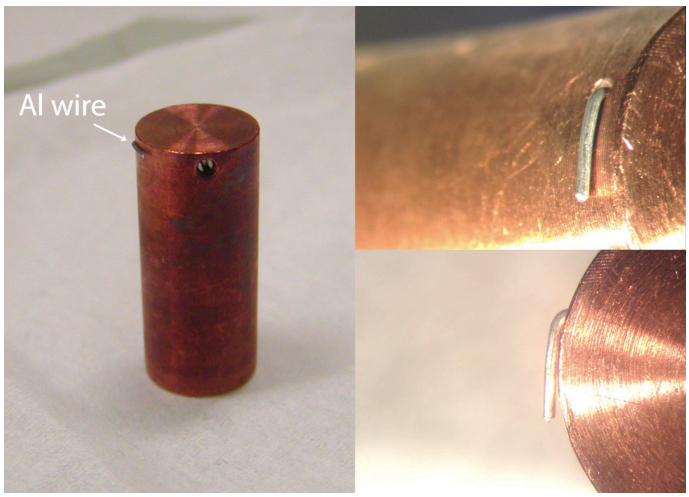

Figure 5. The Al wire used as a substrate for the cells is shown protruding from the Cu cylinder. Insets to the right show the setup from different angles: the top inset is a side view from an oblique angle and the bottom inset is a top view.

4 DEVELOPMENT OF NEW METHODS FOR *IN SITU* ESEM STUDIES

The goal in developing the new methods for *in situ* ESEM studies was to create a versatile experimental platform that could be used for several different types of studies of soft biomaterials, and especially their interaction with water. Two main application areas inspired the design of the platform, namely the controlled wetting of materials with focus on liquid water transport, and the real-time measurement of swelling of hydrated materials with high accuracy.

The developed platform, which we shall call the *in situ* sample stage, consists mainly of a nanomanipulation system, a solution for local cooling by means of the Peltier cooling stage of the ESEM, and a fixture to make the setup compatible with the cooling stage. Depending on the purpose at hand, it can be used in different ways, either for controlled wetting or *in situ* measurements of swelling. To accomplish the latter, a piezoresistive AFM sensor was coupled to the nanomanipulation system, enabling the measurement of forces in the nanoNewton range. The force reading can be converted to sample expansion using the spring constant of the AFM cantilever.

Two different applications were chosen to test and evaluate the performance of the new technique, namely controlled wetting of individual cellulose fibres and measurement of the osmotic response in single yeast cells.

This chapter outlines the corner stones of the development work and describes the hardware setup as well as the experimental methodologies related to the investigations on cellulose fibres and yeast cells.

4.1 The *in situ* sample stage

4.1.1 Overview

Figure 6 shows photos of the *in situ* sample stage in its two configurations: for controlled wetting in (a) and for AFM measurements in (b). With reference to the numbers in the images, the main parts are

1. Aluminium fixture
2. Nanomanipulator
3. Copper cylinder
4. AFM sensor
5. Aluminium wire as specimen holder

Numbers 1-4 will be described in greater detail in the following sections. In addition, an external pressure gauge connected to the microscope sample chamber was used for recording pressure variations in the measurements on yeast cells, but will not be described further.

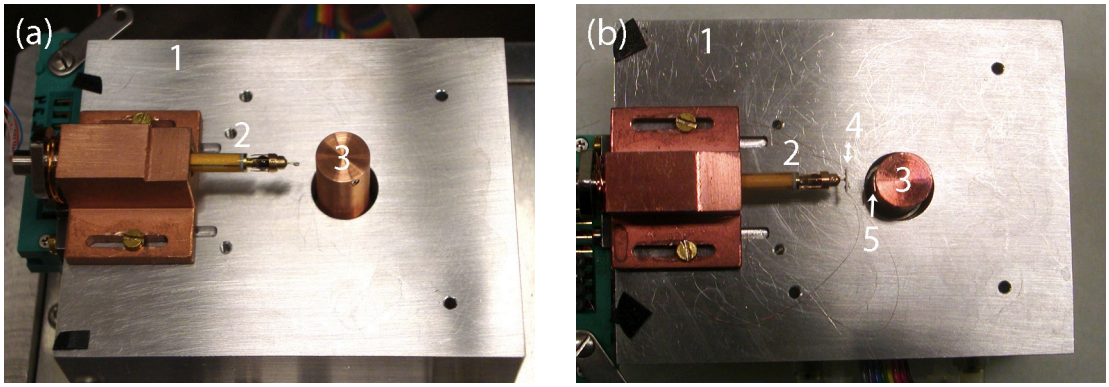

Figure 6. Photos of the in situ sample stage in its two different configurations: (a) for controlled wetting, and (b) for AFM measurements. The main parts are numbered according to the list in this section.

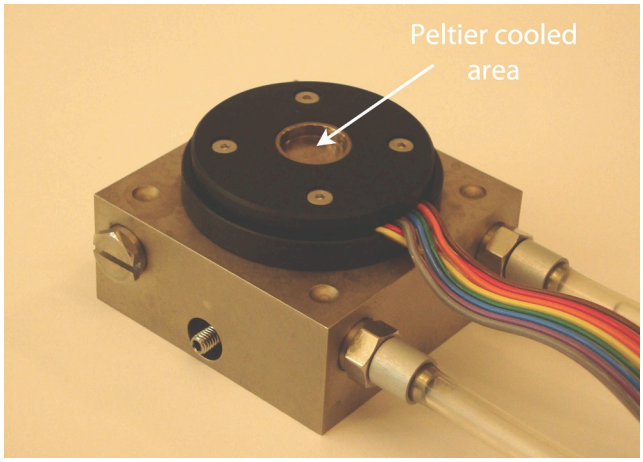

Figure 7. The Peltier cooling stage of the FEI Quanta 200 FEG ESEM, with the cooled area highlighted.

There is yet another important part of the instrumentation that is not visible in the images – namely the Peltier cooling stage, shown in Figure 7. In both configurations, the Al fixture is clamped on top of the cooling stage and the Cu cylinder is placed in contact with the cooling stage through an opening in the fixture. The thermal contact between the cooling stage and the fixture is poor. Consequently, the Cu cylinder is the only part that is actively cooled, and the rest of the setup remains closer to room temperature. This is important, as we want to avoid excessive thermal loading of the Peltier element.

Figure 6(a) displays the controlled wetting configuration of the *in situ* sample stage (paper I). The specimen is situated on the nanomanipulator and on the other side, on the wall of the cooled Cu cylinder, are water droplets acting as reservoirs for wetting of the specimen. Figure 8 illustrates the basic working principle, where the manipulator is used to bring a cellulose fibre in contact with a water droplet. The geometry of this setup provides a clear view of the point of contact between the specimen and the water. Moreover, the difference in temperature between the specimen and the Cu cylinder plays an important role here. This is what gives rise to a difference in relative humidity between the water and the specimen prior to contact, since the water vapour pressure is constant throughout the chamber. The difference in relative humidity, in turn, is

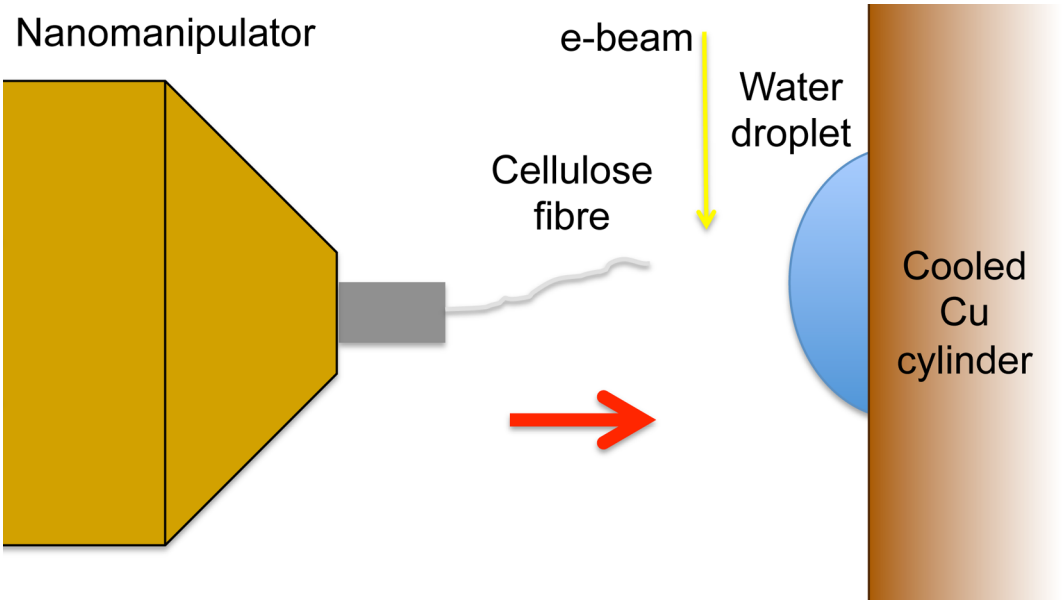

Figure 8. Schematic illustration of the setup used for *in situ* controlled wetting of individual cellulose fibres in the ESEM.

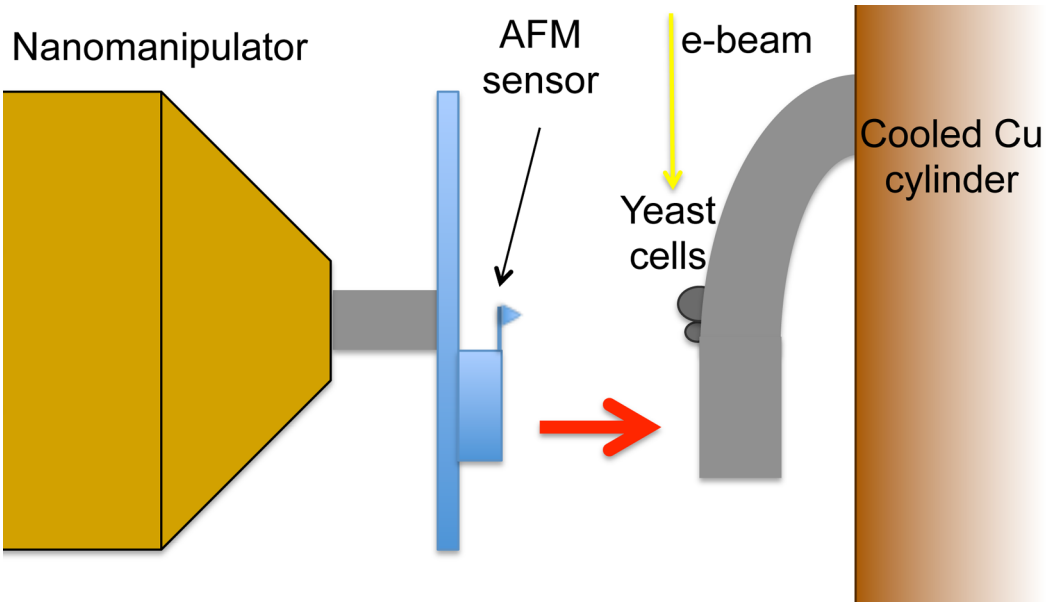

Figure 9. Schematic illustration of the setup used for measuring the osmotic response of single yeast cells in the ESEM.

the basis for the experiment as we are interested in what happens when the specimen goes from comparatively dry to wet.

The ESEM-AFM configuration of the *in situ* sample stage (paper II) is displayed in Figure 6(b). Here, the specimen is located on the Cu cylinder, or rather on an Al wire protruding from the cylinder as shown earlier in Figure 5. The nanomanipulator is occupied by the AFM sensor, which is used to probe the specimen. This is schematically illustrated for yeast cells in Figure 9. In contrast to the controlled wetting configuration, the specimen is cooled in order to be able to control its relative humidity. In the case of the yeast cells, this is essential to their survival in the ESEM.

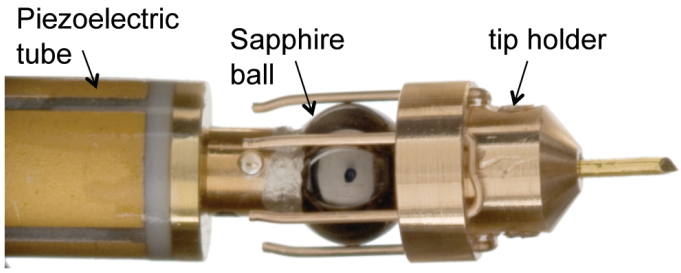

Figure 10. The nanomanipulator with its main parts: the piezoelectric tube, the sapphire ball and the movable tip holder.

4.1.2 Nanomanipulator

The nanomanipulator, shown in Figure 10 is a key constituent of the *in situ* sample stage. It has been developed and produced by Nanofactory Instruments AB (Gothenburg, Sweden) and has a compact design as it was originally built for use inside the transmission electron microscope (TEM). The main parts of the manipulator are:

- a piezoelectric tube with four electrodes on its surface
- a sapphire ball attached rigidly to the piezo tube
- a movable part with six springy legs gripping the sapphire ball

The movable part holds a tip where a sample (or the AFM sensor) can be placed and will henceforth be referred to as the *tip holder.*

This setup enables both coarse and fine movement in three dimensions. The coarse movement is accomplished through inertial sliding of the tip holder against the sapphire ball when applying short voltage pulses to the piezo tube in rapid succession. This mechanism is capable of steps down to 0.1 μm and the stepping speed is tuneable. With a total range of approximately 1 mm it is very useful for aligning the tip against a selected feature during experiments. The expansion and contraction of the piezoelectric tube with applied voltage can be used to fine-tune the alignment on the nanometre length scale. For a detailed description of the nanomanipulator, see (Svensson, Jompol, Olin, & Olsson, 2003).

4.1.3 Aluminium fixture

Part of the development work was to design a fixture that could make the rest of the instrumentation compatible with the Peltier cooling stage of the microscope. There were several design requirements to take into account. Firstly, the fixture should accommodate the nanomanipulator and its housing. Electrical connections for the signal input and output also had to be fitted on the fixture, with further connections to the microscope chamber feedthrough. Secondly, the fixture should provide access to the cooled area of the cooling stage underneath it. Third, it should be easy to fit over the cooling stage, yet thermally insulated from it to avoid excessive thermal loading of the Peltier element. Ultimately, all of this must be accomplished in the constricted space inside the microscope chamber.

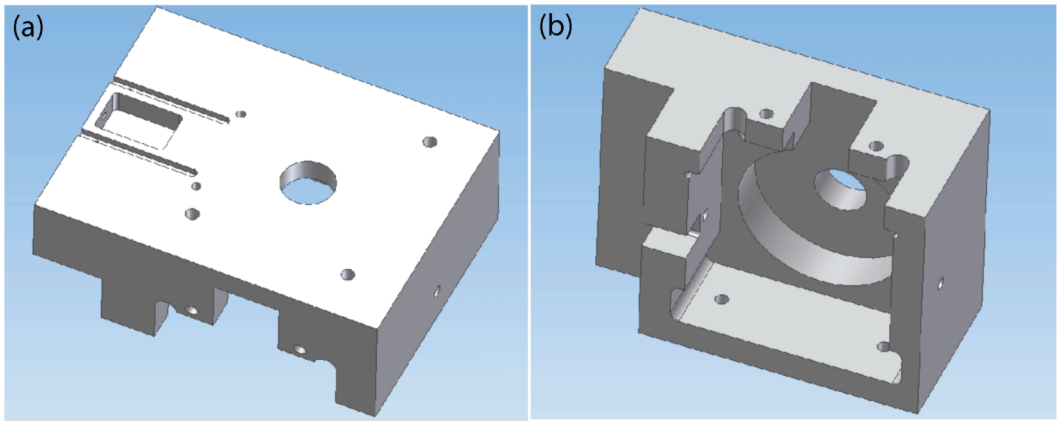

Figure 11. CAD drawing of the Al fixture, viewed from the top (a) and from the bottom (b). The shape is designed to fit over the Peltier cooling stage shown in Figure 7, and the central opening provides access to the Peltier cooled area of the cooling stage.

Our solution is shown in the form of a CAD drawing of the fixture in Figure 11 (a) and (b). The milled structures on the left part of the fixture in (a) are where the manipulator is installed. The bottom view in (b) shows that the fixture is tailor made to fit the shape of the cooling stage (see Figure 7 for a view of the cooling stage). Furthermore, it is locked into place nylon screws that create an air gap between the two parts, preventing heat conduction from the fixture to the cooling stage. The hole in the centre provides an opening for accessing the Peltier cooled area. Terminals for electrical connections are not included in the figure.

4.1.4 Copper cylinder

As explained in section 4.1.1, the *in situ* sample stage has two configurations to enable both controlled wetting experiments and force measurements related to swelling of hydrated materials. Both cases require a solution for local cooling of a site readily accessible to the nanomanipulator. To this end, we used a cylindrical block of solid copper (Cu) with a high purity for optimal heat conductance. The cylinder had a height of approximately 20 mm to match the height of the nanomanipulator and a width of 9.5 mm corresponding to the size of the Peltier cooled area on the cooling stage. This solution provided a simple geometry that would fit the demands of the two types of application, as well as sufficient heat conductance to create a cold site 20 mm away from the actively cooled area on the cooling stage.

An important aspect in relation to this is the thermal equilibration throughout the Cu cylinder. In paper I, it was found that the temperature at the top of the cylinder was equal to that at the bottom after a few minutes, indicating thermal equilibration. In paper II, an Al wire was fastened inside a slot in the Cu cylinder and the part protruding from the cylinder was used as a sample holder as explained in section 3.2.2. A photograph of this arrangement was shown in Figure 5. The temperature at the surface of the Al wire was found to differ by approximately 1°C from that of the Cu cylinder. This may be explained by the small contact area between Al and Cu inside the slot in the cylinder, the comparatively poor heat conductivity of Al and the fact that the wire was

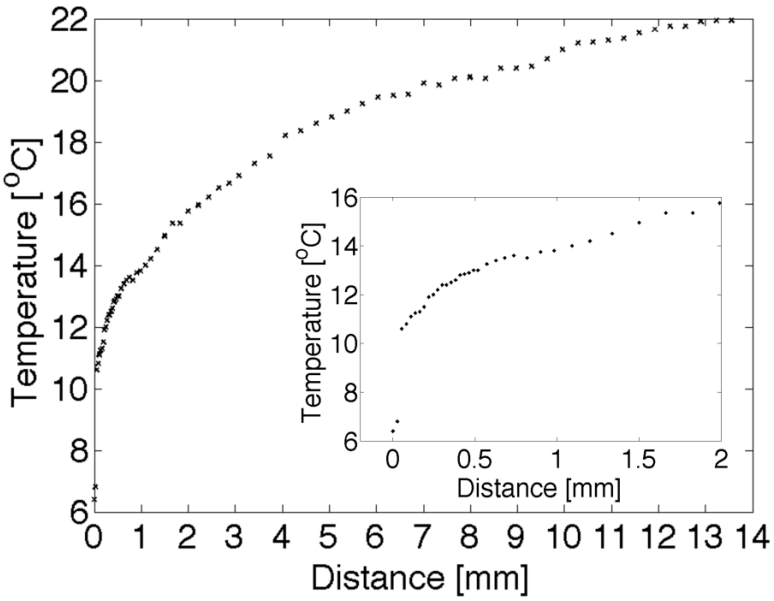

Figure 12. The temperature as a function of distance to the wall of the Cu cylinder. The cylinder was kept at 1°C, and the discrepancy in the temperature at contact may be explained by the small contact area between the cylinder and the measuring device.

protruding from the cold cylinder. It is important to be aware of the discrepancy in temperature when calculating the relative humidity at the sample site.

For the *in situ* controlled wetting experiments, it is also important to be aware of the temperature gradient that prevails in the vicinity of the cold Cu cylinder. The temperature was measured as a function of distance from the vertical wall of the cylinder using a type K thermocouple. The temperature of the cylinder was kept at 1°C and the pressure at 4.93 torr corresponding to the conditions used in the *in situ* controlled wetting experiments. Figure 12 displays the result, with an inset showing a close-up of the region closest to the cylinder. It is clear that the temperature decreases as the cylinder is approached and that the gradient steepens. The temperature measured at contact was approximately 6°C. It differs from the expected 1°C, probably due to the very small contact area between the surface of the spherical thermocouple junction and the wall of the cylinder. The implications of the temperature gradient will be discussed later in section 5.3.1.

4.1.5 AFM sensor

The AFM sensor used in the experiments was developed and characterised by Nafari and co-workers, and has an on-chip integrated Wheatstone bridge for piezo-resistive signal transduction (Nafari, 2008). This microelectromechanical (MEMS) sensor features a cantilever with a pyramidal tip for probing the specimen. The bandwidth of the electronics is 5 kHz to enable recording of events on the millisecond time scale. For a detailed account of the properties of the AFM sensor the reader is referred to (Nafari, Karlen, Rusu, Svensson, Olin, & Enoksson, 2008).

The AFM sensor was provided by NanoFactory Instruments AB, and the value of the spring constant of the cantilever was given by the manufacturer as 2.8 N/m. To integrate the sensor with the *in situ* sample stage, the printed circuit board of the sensor was glued to an Al wire that fitted into the tip holder of the nanomanipulator. To transfer the signal from the sensor to the read-out electronics, four Cu wires with a thickness of 50 μm were soldered to the backside of the sensor's printed circuit board and led to a terminal of electrical contacts on the side of the Al fixture. The wires had to be thin and long enough not to obstruct the movement of the tip holder during operation of the nanomanipulator.

The output from the AFM sensor is a voltage that is translated by a software programme into a force using known parameters for the spring constant of the cantilever and the electrical sensitivity of the sensor (Nafari, 2010). Two different types of force measurements can be performed. The first is simply a log of the force registered by the sensor over time. This is used to measure the expansion of individual yeast cells as a result of increased relative humidity in paper II. The other type of measurement is a force-displacement curve produced by the sensor approaching and then retracting from the specimen, thus loading and unloading the cantilever. This method was used to probe the Young's modulus of the yeast cells in paper II.

4.2 *In situ* controlled wetting of individual cellulose fibres

The experimental setup for *in situ* controlled wetting is shown in Figure 6(a) above. The idea behind this method is to monitor the interaction of the specimen with liquid water by simultaneous imaging and manipulation. Structural changes typically take place as the material goes from dry to wet and, depending on the nature of the specimen, swelling and transport of water may occur.

Figure 8 schematically shows the principle of the experiment, where the nanomanipulator is used to bring a fibre in contact with a water droplet formed on the vertical wall of the Cu cylinder. Here, the setup is viewed from the side for clarity, but the electron beam used for imaging is incident from above and thus creates an image where the specimen and the water droplet are viewed from above.

The method used for *in situ* controlled wetting of individual cellulose fibres can be described as follows. Before the experiment could begin, a few preparation steps were required. The Cu cylinder was cooled to 1°C and a few minutes were allowed for thermal equilibration. During this time, the tip holder with a single cellulose fibre was mounted and a coarse alignment with respect to the Cu cylinder was performed. By moving the housing of the nanomanipulator, the tip of the fibre was positioned about 1 mm from the edge of the Cu cylinder. This was a suitable distance considering the range of movement of the nanomanipulator and the relative humidity of the sample at the start of the experiment, which was estimated to approximately 30% based on the temperature data presented in Figure 12.

Next, the microscope chamber was pumped to operating pressures using a built-in protocol that gradually exchanges air for water vapour without purging the microscope chamber (Dufek & Hayles, 2003). The starting water vapour pressure was set to 3.75 torr. For 1°C condensation occurs at a pressure of 4.93 torr. An acceleration voltage of 5 kV was used for imaging, as our previous observations had shown no signs of beam damage to the yeast cells at this voltage. The working distance was 5-6 mm. Water droplets were formed on the cold Cu cylinder by increasing the pressure to slightly above the condensation point. When the droplets had grown to a suitable size, the pressure was lowered to the condensation point to stabilise the droplets.

The specimen was brought into contact with a suitably located water droplet using the inertial sliding coarse movement of the nanomanipulator. Focusing on the edge of the droplet, alignment in the direction of the electron beam was performed by adjusting the height of the specimen until it came into focus. The wetting process was then recorded in the form of a movie using a frame rate of 5 images/second.

4.3 Single yeast cells' stiffness and response to osmotic shock

The experimental setup for *in situ* force measurements on single yeast cells was shown in Figure 6(b). The main purpose of this method is to probe the swelling of cells due to an increase in relative humidity, although the approach can be extended to other hydrated soft materials. The humidity increase is accomplished by raising the water vapour pressure in the sample chamber. This increases the concentration of water molecules outside the cell, and the assumption here is that it creates a situation analogous to a hyposmotic shock, i.e. a net influx of water into the cell across the cell membrane. The resulting change in size of the cell can be measured with high accuracy and temporal resolution using the AFM sensor. This principle is illustrated in Figure 9.

4.3.1 Experiment

The method used can be described as follows. The AFM sensor was mounted on the tip holder of the nanomanipulator and its electrical contacts were connected to the control system. The *P. pastoris* yeast cell sample was prepared as outlined in section 3.2.2. The Cu cylinder, with the Al wire containing the adsorbed yeast cells, was put in place on the *in situ* sample stage. The Peltier cooling stage had been precooled to 1°C and, as mentioned in section 4.1.4, a few minutes of equilibration time had shown to bring the temperature at the specimen site (i.e. the Al wire) to 2°C. A coarse alignment of the sensor cantilever and the sample was made. The preparations were performed as quickly as possible to minimise the exposure of the sample to the environmental conditions of the lab.

The pressure in the microscope chamber was brought to 3.5 torr using the same gradual pump-down sequence with no purge as in the case with the cellulose

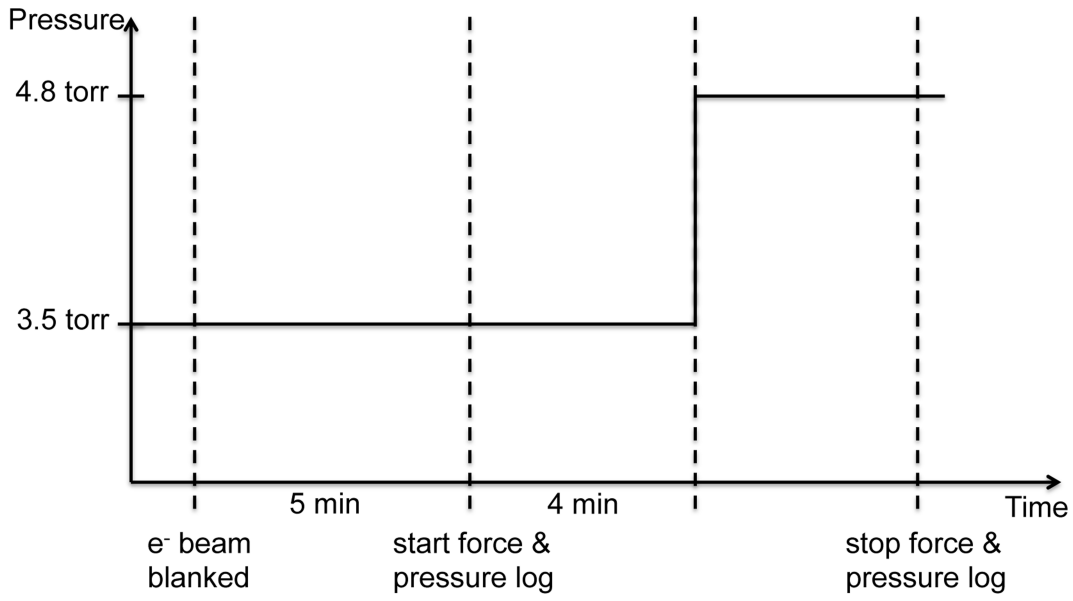

Figure 13. Schematic representation of the experiment on a yeast cell in ESEM.

fibres (see section 4.2). The relative humidity at 2°C and 3.5 torr is 66%. After initiation of imaging at an acceleration voltage of 5 kV and a working distance of 5-6 mm, the nanomanipulator was used to bring the sensor tip into contact with a suitably located yeast cell on the Al wire. Alignment in the direction of the electron beam was performed by focusing on the yeast cell and adjusting the height of the cantilever tip until the tip apex came into focus. To minimise the high magnification imaging of the cell, the alignment procedure was performed at relatively low magnification as far as possible and the beam was blanked at times when imaging was not needed.

Next, the electron beam was blanked to allow stabilisation of the AFM sensor. After 5 minutes, the force reading from the sensor had stabilised and logging of the force output was started. At the same time, logging of the pressure in the microscope chamber was started. The pressure was measured by a pressure gauge connected to the sample chamber as mentioned in section 4.1.1, and recorded using an oscilloscope. After a baseline of 4 minutes had been acquired, the pressure was raised to 4.8 torr, which at 2°C corresponds to 90% relative humidity. The force and pressure were logged for another few minutes until the force reading appeared to have stabilised. A schematic representation of the experiment is shown in Figure 13.

The same experiment was performed on the surface of the Al wire, i.e. the substrate on which the yeast cells were located, soon after the measurement on the yeast cell was completed. The purpose was to obtain a reference curve that would be subtracted from the yeast cell curve in subsequent data analysis, to compensate for movement of the substrate in connection to the pressure change. Such movements could be the result of e.g. thermal expansion of the Cu cylinder and/or Al wire due to increased impingement of water molecules upon pressure increase. The reference measurement was performed in close proximity to the chosen yeast cell, with the sensor tip contacting the surface of the Al substrate.

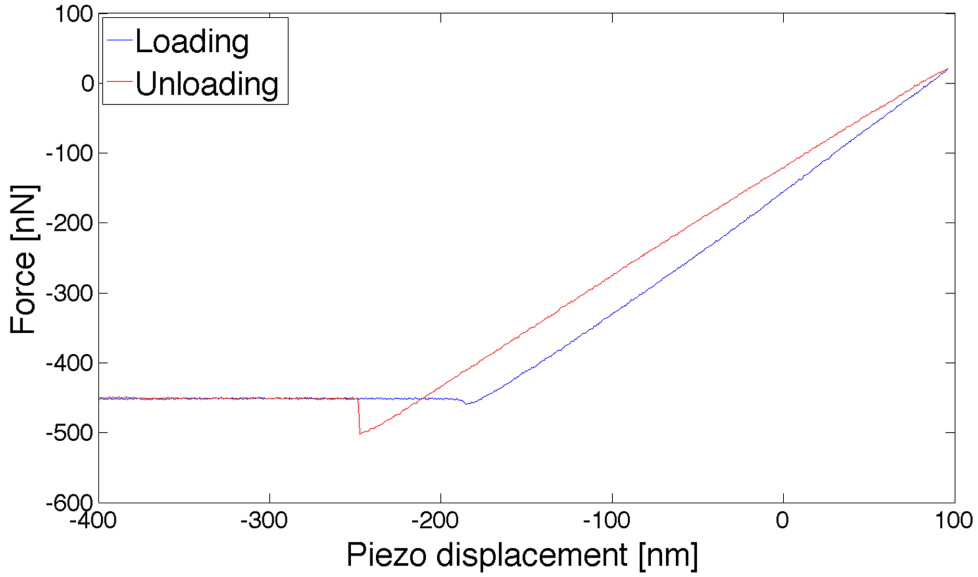

Figure 14. Example of a force-displacement curve obtained on a yeast cell at 66% relative humidity in the ESEM.

4.3.2 Data analysis

As mentioned in section 4.1.5, we can perform two different types of measurement using the AFM sensor. In paper II, this was explored to obtain the following results:

- the Young's modulus of cells at 66% relative humidity, and
- the cellular expansion due to osmotic shock in the ESEM.

The calculation of Young's modulus is based on curves of force vs. piezo displacement where the sample is indented to an extent depending on its stiffness. An example of a force-displacement curve for a *P. pastoris* yeast cell is shown in Figure 14. It is linear and features a snap-out effect, visible in the unloading part of the curve.

Young's modulus for a single yeast cell was calculated by transforming the piezo displacement to sample indentation using the cantilever deflection on a hard undeformed surface, as in e.g. (Weisenhorn, Khorsandi, Kasas, Gotzos, & Butt, 1993). The resulting force-indentation curve was then fitted to the Sneddon model for a cylindrical indenter. This model was chosen based on the relatively large indentation depth and the presence of adhesion effects, which precludes the use of the Hertz model for a spherical indenter. The cylindrical indenter model is linear, which agrees with the shape of our experimental force-indentation curves. Here, the force F acting on the cell is then described by

$$F = 2R\frac{E}{1-\nu^2}\Delta z$$

where E is the Young's modulus of the cell, R the radius of the probe tip, ν the Poisson's ratio of the cell and Δz the indentation depth (Weisenhorn, Khorsandi, Kasas, Gotzos, & Butt, 1993). ν can be assumed to be 0.5 for a soft biological

material (Lanero, Cavalleri, Krol, Rolandi, & Gliozzi, 2006). The Young's modulus was extracted from the coefficient.

The cell expansion due to osmotic shock was obtained from the force measured by the AFM sensor through the pressure change experiment, which was logged over time by the control software. The force was transformed to displacement of the AFM tip using the spring constant of the cantilever. The temporal correlation of the cell expansion curve with the pressure curve was sorted out using time stamps contained in the raw data files. The complete length of the baseline acquired before the pressure step in the experiment is not shown in the final presented plot.

5 *IN SITU* CONTROLLED WETTING OF INDIVIDUAL CELLULOSE FIBRES

The *in situ* sample stage was used for controlled wetting of individual cellulose fibres in paper I. The purpose was to evaluate the performance of the method and to obtain qualitative results illustrating the possibilities of this new approach. This chapter summarises the results and assesses the performance of the developed technique.

5.1 Summary of results

An ESEM image of an individual cellulose fibre is shown in Figure 15(a). This fibre belonged to the mercerised batch and was cut using scissors to expose the central cavity, or *lumen*, that is visible in the image. For this particular specimen, the lumen appears to be open rather than collapsed. When several different fibres were examined with respect to their overall shape and structure, there was a considerable variation in the degree of collapse of the lumen and the tortuosity of the fibre. This probably reflects the mixed origin of the fibres in the batch where the samples were taken (see section 3.2).

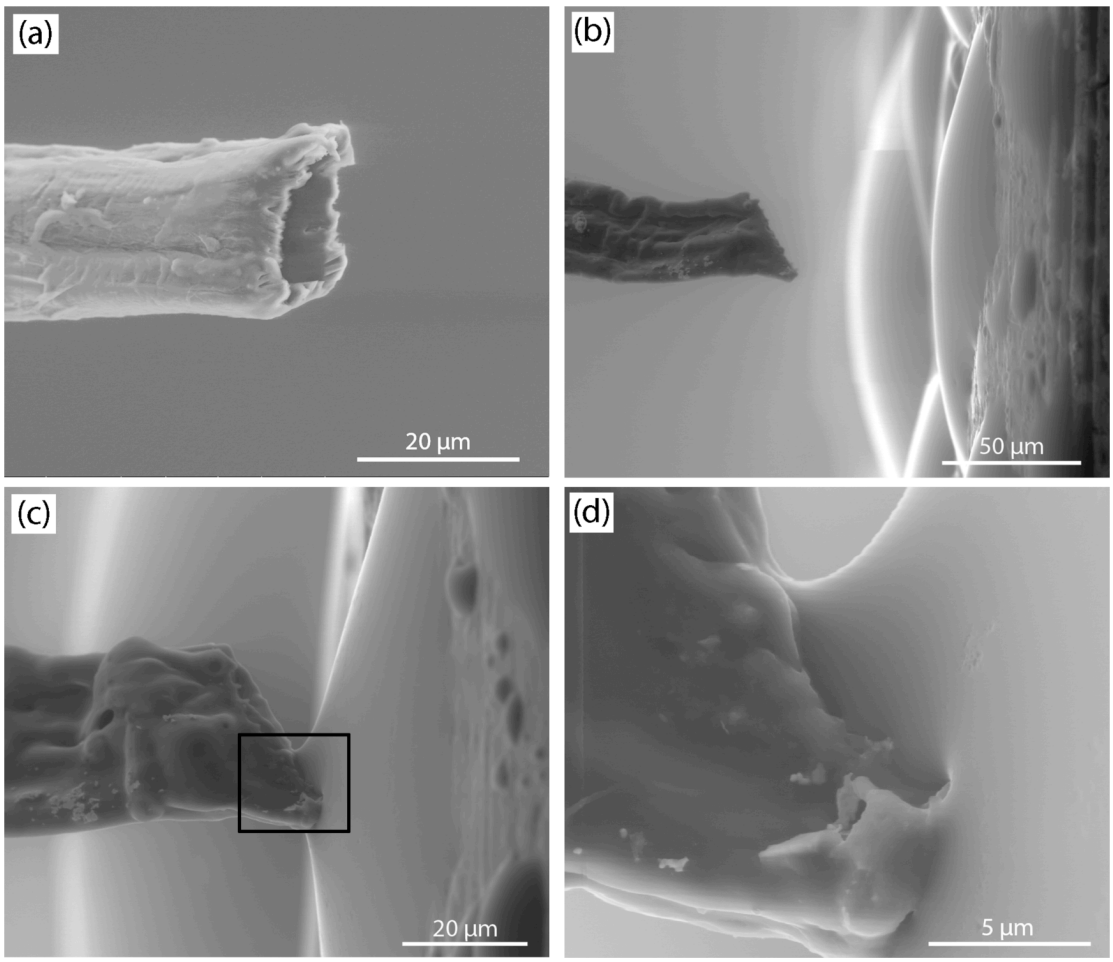

Figure 15. (a) ESEM image of an individual (mercerised) cellulose fibre. The tip was cut using scissors to expose the lumen. (b)-(d) ESEM images of a cellulose fibre approaching and making contact with a water droplet on the vertical wall of the Cu cylinder. The point of contact, highlighted by a box in (c), is shown at a higher magnification in (d).

The *in situ* controlled wetting experiments were carried out according to the procedure outlined in section 4.2. Figure 15(b)-(d) shows an example where a cellulose fibre makes contact with a water droplet on the vertical wall of the Cu cylinder, and the point of contact between the fibre and the droplet can be clearly seen. Swelling of the fibre was generally observed as an increase in thickness and a smoothening of surface topography. Much of the swelling was observed to take place during approach toward the cylinder, prior to contact with the liquid water.

The series of images displayed in Figure 16 shows how an entire water droplet shrinks and disappears as it is put in contact with an individual cellulose fibre for an extended period of time. The images are selected frames from a movie that shows how the fibre swells before reverting back to its original shape. Arrows in the images of Figure 16 highlight this change in shape. The results indicate that the water droplet was absorbed and transported away from the surface of the Cu cylinder by the fibre. Several supporting arguments for this interpretation are presented in paper I. Moreover, the duration of the absorption process was about 15 s and the droplet volume was estimated to approximately 0.02 nL.

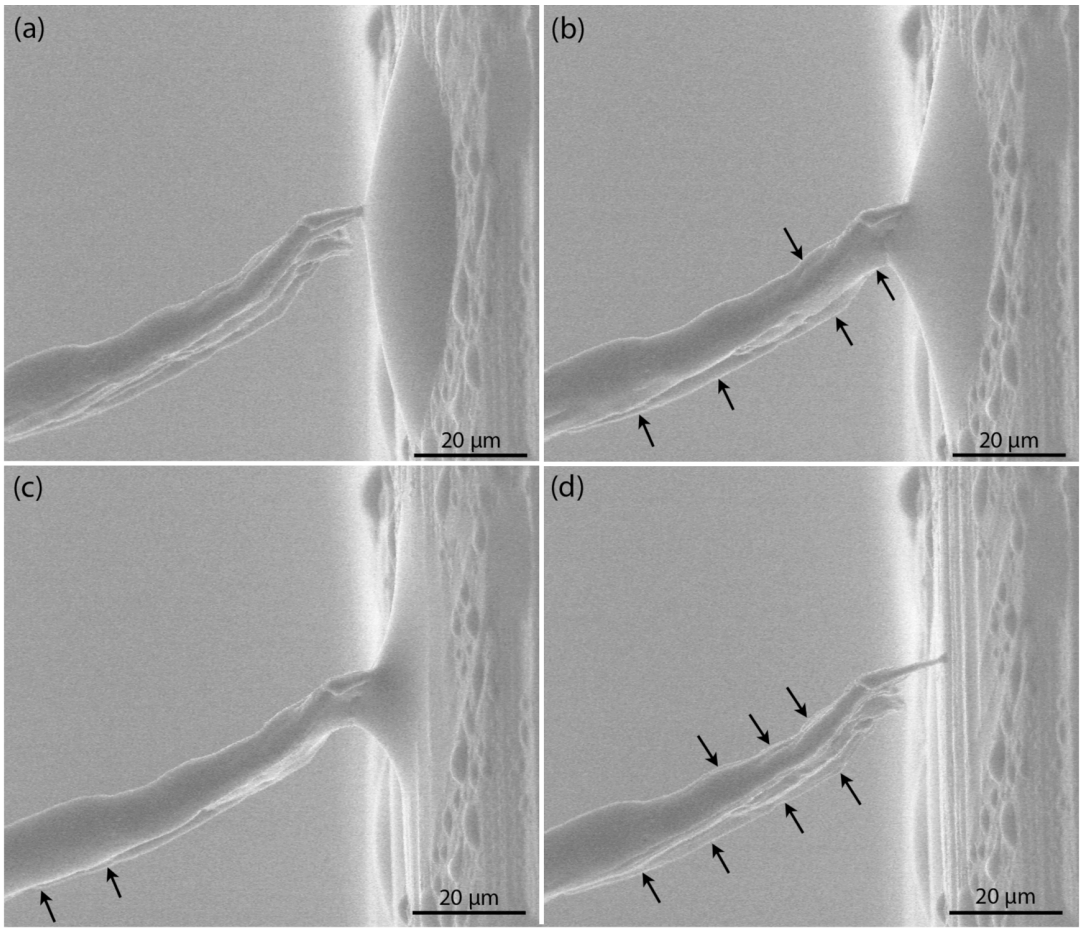

Figure 16. ESEM images from a movie showing how an individual cellulose fibre absorbs and transports a water droplet away from the surface of the Cu cylinder. During the process, the fibre shape changes as highlighted by arrows. It swells and then reverts back to its original shape.

The experiment was repeated with several individual fibres, exhibiting a variation in absorptive capacity with respect to the time of absorption for different sized droplets as well as the number of droplets that could be absorbed in series before saturation was reached. Again, the mixed origin of the fibres in the batch from which the samples were taken is believed to be the reason for this variation, as it may affect factors relevant to the absorptive capacity such as e.g. length, width, tortuosity and size/accessibility of lumen.

5.2 Comment on the respective roles of cell wall and lumen

As an addendum to paper I, the literature review on water-fibre interaction in section 2.1.2 in combination with the temperature data presented in section 4.1.4 may be used to comment on the respective roles of the cell wall and the lumen in the *in situ* controlled wetting experiments. Figure 9 displayed the variation of temperature with the distance to the cold Cu cylinder. At 1 mm, which was approximately the maximum distance between the tip of the cellulose fibre and the Cu cylinder at the start of the experiment, the temperature is about 14°C. The water vapour pressure was initially 3.75 torr and was then increased to almost 5 torr to condense water onto the cylinder. The relative humidity can then be estimated to 30% at 3.75 torr and 40% at 5 torr. During approach toward the cylinder, the temperature decreases and the relative humidity increases toward 100% just before contact with the liquid water.

As mentioned in the previous section 5.1, some swelling of the cellulose fibres was observed prior to contact with the liquid water in the *in situ* ESEM experiments, which is to be expected with increasing moisture content below the fibre saturation point (FSP). According to tables of the equilibrium moisture content (EMC) of wood (see e.g. (Bergman, et al., 2010)), the moisture content increases from approximately 6% to 25% as the relative humidity increases from 30% to 95% at the temperatures used. It should be noted that these are equilibrium values and that wood may take a long time to reach equilibrium at constant relative humidity and temperature. However, the time for moisture content equilibration decreases with decreasing size of the wood piece (Rowell, 2012) and hence, for a single cellulose fibre, it is likely to be insignificant on the time scale of the experiment. Furthermore, it would be a reasonable first assumption that the numbers given in EMC tables for wood are approximately valid also for individual cellulose fibres. If anything, the moisture content at the corresponding relative humidity should be higher than for wood, considering the absence of the relatively hydrophobic lignin component, which is largely removed in the pulping process, and the fact that in the ESEM, the lumen is filled with water vapour instead of air.

On the basis of these assumptions, we can consider the implications of the FSP. As mentioned in section 2.1.2, the FSP is generally quoted to around 30%, although the value does vary somewhat (Bergman, et al., 2010). This is rather close to the moisture content just before contact with the liquid water, as estimated above. Hence, the cell wall can be considered close to saturation just before contact with the water. Therefore, we suggest that the water transport

observed to take place through the fibre after contact (e.g. in Figure 16) be mainly attributed to capillary forces in the lumen.

5.3 Evaluation of the method

This section evaluates the performance of the new *in situ* ESEM method for controlled wetting of materials on the basis of the experiments with individual cellulose fibres summarised in this chapter.

5.3.1 Practical aspects of the in situ *ESEM experiment*

The positioning of the specimen could be accurately controlled using the nanomanipulator, and alignment with the water droplet in the direction of the electron beam was accomplished by bringing both objects into focus at the same time as described in section 4.2. The minimum working distance was limited by the size of the tip holder. A distance of about 5 mm to the pole piece (which is <5 mm from the final pressure limiting aperture of the gaseous secondary electron detector) was regarded as the minimum "safe" distance, i.e. without risk of crashing into the detector.

The size of the water droplet used as a reservoir for wetting of the fibre could be controlled to an extent through the choice of droplet, but also through the water vapour pressure. The pressure can be used to induce a general growth or shrinkage of the droplets at any time. However, at the later stages of approach when the specimen is close to the Cu cylinder, caution should be taken with regard to such adjustments in order to keep the moisture content of the specimen stable. It is advisable to take a few images of the specimen before and after formation of the water droplets, to be able to spot any differences in the appearance due to the change in relative humidity.

The wetting process was captured by movie recording and images. Movies were recorded at a frame rate of 2-5 s^{-1}. The frame rate is limited by the scanning speed of the electron beam, which is in turn limited by the minimum acceptable signal-to-noise ratio. In other words, there is a trade off between temporal resolution and signal-to-noise ratio. For the particular processes observed in connection to the wetting of the individual cellulose fibres, the temporal resolution at the frame rates used was sufficient.

An important aspect concerns the increasing relative humidity of the specimen during the course of the approach toward the cold Cu cylinder, as discussed in section 5.2. The observed swelling of the fibres prior to contact with the liquid water indicates that the fibres are affected by the humidity gradient, which arises because of the temperature gradient near the cylinder. This behaviour cannot be expected to accurately represent the real conditions in applications of the material, e.g. in absorbents where the exposure to moisture is more sudden and there is no pre-swelling of the fibres. However, it is a considerable improvement compared to the traditional way of conducting wetting experiments in the ESEM, where water droplets are gradually formed on the specimen surface through pressure increase (or temperature decrease) and water transport cannot be readily observed. If applied to the cellulose fibres

used in this work, the traditional method would simply induce swelling of the fibre wall. It should also be pointed out that the temperature gradient in the vicinity of the cold Cu cylinder has a positive implication, namely to ensure a low rate of evaporation from the fibre close to the point of contact with the liquid water. As a result, evaporation can be regarded a minor influence on the wetting process.

5.3.2 Sample handling and preparation

As always when working with water and materials in the ESEM, one has to consider the hydration state of the specimen at the start of the experiment. This may be affected by the sample handling and preparation prior to the investigation as well as the pump-down procedure used to reach operating pressures in the sample chamber of the microscope. As mentioned in section 3.2.1, the preparation of the single cellulose fibres involved a drying step to cure the epoxy resin used to mount the sample. During this step, the fibres were exposed to dehydrating conditions for a prolonged period of time and, hence, subject to hornification as described in section 2.1.2. This most likely had an effect on the fibre wall structure and, consequently, on its ability to absorb water and swell in the *in situ* ESEM experiments. Since the water content of the sample was very low at the time of insertion into the microscope, the pump-down step (which was carried out according to a gradual no-purge protocol as stated before) probably had only a minor influence, if any.

One can speculate in the possibilities of reducing the exposure to dehydrating conditions during sample preparation and pump-down. However, when it comes to single cellulose fibres, it is doubtful if any alternative procedure could have maintained the moisture content of the fibre as it was in the never-dried pulp. The reason is that the rate of drying of a single fibre, some 20-30 μm in diameter, should be high due to the large surface-to-volume ratio. The sole process of extracting an individual fibre from the pulp and mounting it on some sample holder takes at least a couple of minutes, during which time the fibre most likely suffers some extent of hornification. Ultimately, we can deduce from the experimental results that the fibre obviously retained some swellability, and that despite probable hornification effects, it is possible to study water transport in individual cellulose fibres using the developed technique. However, in comparative studies of the transport properties of fibres, e.g. for fibres with different processing history, it is important to make sure that the sample handling and preparation is as standardised as possible. A possible way of circumventing the problem could be to perform a solvent exchange of the never-dried pulp, after which the pulp can be dried in a special manner to avoid hornification, see e.g. (Köhnke, Lund, Brelid, & Westman, 2010).

5.3.3 Applicability to cellulose fibres and other materials

When applying the new method for *in situ* controlled wetting to cellulose fibres, it is important to remember the conditions under which the experiments were carried out – in particular when considering the *rate* of absorption of liquid water by the individual cellulose fibres in the ESEM. Individual fibres were cut to expose the lumen, and the geometry was chosen to give absorption in the longitudinal direction of the fibre, i.e. along the direction of the lumen. Also, prior

to contact, the lumen was filled with water vapour at a low pressure (5 torr). As stated in section 2.1.2, the absorption rate is highest in the longitudinal direction and the absorption rate is affected by the rate at which air can escape the lumen to be replaced by water. The work required to expel low pressure water vapour might differ from the "normal" situation with air at atmospheric pressure.

Nevertheless, our method is an interesting break from the traditional ways of studying the interaction between cellulose fibres and water. For the first time, direct and visual information on how water is absorbed by a single, isolated cellulose fibre in real time is available. As previously mentioned, water absorption in a network of fibres is a complex matter, with contributions from porosity and capillary spaces between the fibres as well as from the individual fibres themselves. Therefore, studying a fibre in isolation is valuable for the understanding of the fundamental aspects of the interaction. Effects of hornification upon cyclic drying and rewetting could be studied from a new

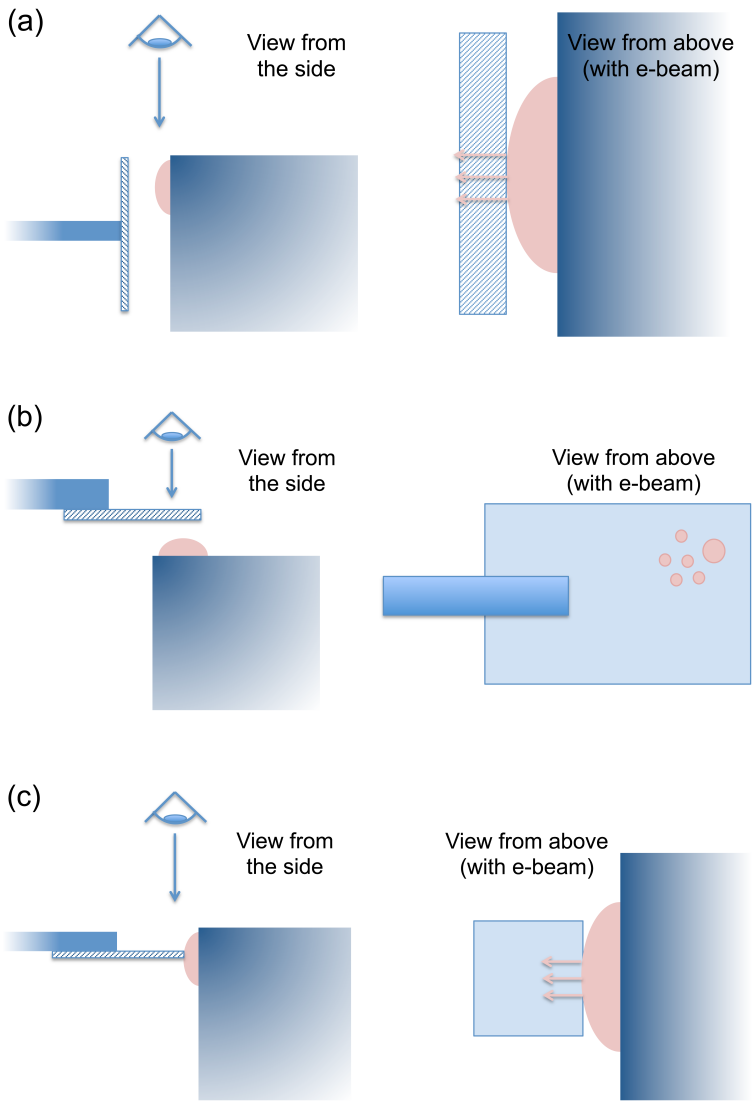

Figure 17. Adaptation of the method for *in situ* controlled wetting to the study of water transport through thin suspended films. Three different sample orientations are schematically displayed in (a), (b) and (c). The pink-coloured parts represent the water. The application to thin polymer films is being explored in on-going work.

perspective. Moreover, comparative studies of different phenomena could yield important information. For example, one could investigate how different processing conditions affect the transport properties of fibres, or how the transport varies in different directions of the fibre.

Lastly, a comment on the applicability of the developed *in situ* ESEM technique to other materials. The geometry of the setup in Figure 8 is suitable for the case of a fibre and certainly for several other types of specimens as well. However, there is some flexibility with respect to the geometry of the specimen-water interaction allowing different solutions depending on the type of sample and the purpose of the experiment. Consider for instance a suspended thin film, where the transport of water through the film is of interest. Several alternative geometries can be employed to investigate the transport properties of the film in different ways, as shown in Figure 17. The film can be arranged vertically as in (a) to make contact with a water droplet sitting on the edge of the Cu cylinder while imaging the water transport through the film cross section from above. In another scenario in (b), the film can be arranged horizontally and be lowered toward a water droplet situated on the top surface of the cylinder with its bottom flat surface making contact. This way, the penetration of water through the opposite surface of the film can be imaged. Yet another arrangement can be imagined, where the film is horizontal and again makes contact with a water droplet on the edge of the cylinder, as in (c). This enables the observation of lateral water transport through the film. Similarly, the geometry should be considered for each new material and type of investigation, to explore possible solutions for the particular problem at hand.

6 SINGLE YEAST CELLS' STIFFNESS AND RESPONSE TO OSMOTIC SHOCK

In paper II, the *in situ* sample stage was used for experiments on single *P. pastoris* wild-type yeast cells in the ESEM. The purpose was to verify a method for quantitative evaluation of the expansion of an individual yeast cell due to osmotic shock. Here, we assume that an increase in relative humidity around the cell creates a situation analogous to a hyposmotic shock, where water migrates into the cell across the cell membrane due to the increased concentration of water molecules on the outside.

The *in situ* experiments were performed according to the method outlined in section 4.3. The humidity increase was accomplished in the ESEM by increasing the water vapour pressure at constant sample temperature. Cell size changes were measured using the AFM sensor and correlated with the changes in pressure. In addition, Young's moduli of yeast cells were extracted from force-displacement curves. This chapter summarises the results and assesses the performance of the technique.

6.1 Summary of results

The AFM tip was brought in contact with individual yeast cells on the Al substrate. Figure 18 shows an ESEM image of a yeast cell in contact with the AFM tip. A few other cells are also visible in the image.

The expansion due to osmotic shock was measured for two individual yeast cells. The water vapour pressure was raised from 3.5 to 4.8 torr, corresponding to an increase in relative humidity from 66% to 90%. The result of the experiment is displayed in Figure 19, where both the expansion and the pressure are plotted as a function of time. The pressure increase results in an expansion of both cells,

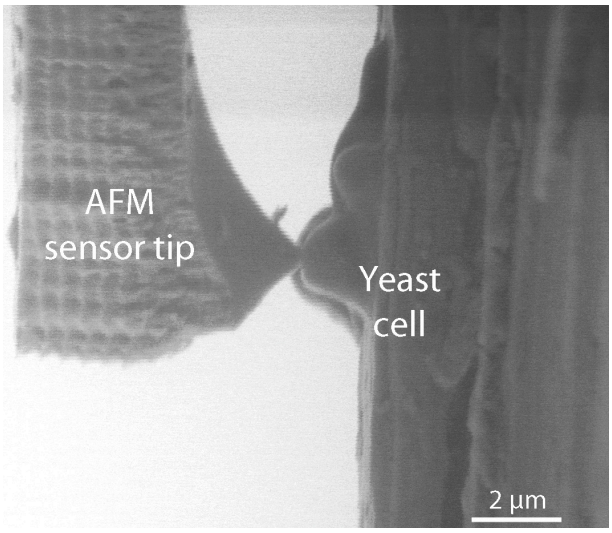

Figure 18. ESEM image of a yeast cell in contact with the AFM tip at 66% relative humidity. The cell has a *bud* (daughter cell) that can be seen next to it in the image, and a few other cells are also visible behind these two.

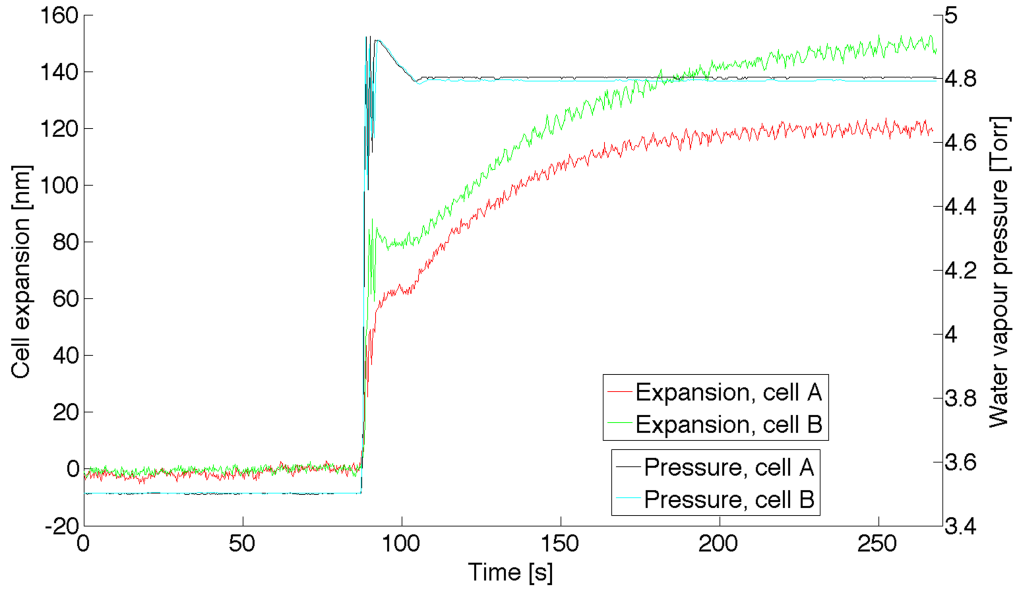

Figure 19. The expansion of two yeast cells A and B as a function of time, and the water vapour pressure as a function of time. The pressure is increased from 3.5 to 4.8 torr at about 87 s, corresponding to a change in relative humidity from 66% to 90%.

which appear to stabilise at 120 and 150 nm expansion, respectively. The response is very fast in the initial stage and follows the pressure peak as the pressure overshoots its target value during the first 20 s. The responses of the two cells thus look qualitatively similar to each other.

The final expansion values were compared with the expansion observed in images of the cells from before and after the experiment. It was found that the expansion measured by the AFM sensor is somewhat higher than indicated by the images. The reason is that the depth of the indentation in the cell wall caused by the pressure from the AFM sensor depends on the Young's modulus which, in turn, depends on the turgor pressure in the cell. The turgor pressure increases as the cell absorbs water and swells. The indentation depth is therefore reduced through the swelling process, contributing to the local expansion measured by the AFM sensor at the point of contact. This effect can be avoided if a cantilever with a low spring constant is used, allowing the AFM tip to follow the cell expansion without indentation.

The Young's moduli of the yeast cells were extracted from force-displacement curves according to the method outlined in section 4.3.2. For cells A and B we obtained Young's moduli of 13 and 15 MPa, respectively. These values are in the same range as earlier results on the yeast *Saccharomyces cerevisiae*, see e.g. (Lanero, Cavalleri, Krol, Rolandi, & Gliozzi, 2006) (Ahmad, Nakajima, Kojima, Homma, & Fukuda, 2007) (Ahmad, 2008) (Ahmad, 2011).

6.2 Evaluation of the method

The purpose of developing the *in situ* ESEM method was to establish a way to accurately monitor the expansion of individual yeast cells as a result of an

increase in relative humidity in the ESEM. This is based on the assumption that an increase in relative humidity is analogous to a hyposmotic shock in the sense that it causes water influx across the cell membrane and consequent cell swelling. The technique was applied to *Pichia pastoris* wild type yeast cells and swelling was observed as the water vapour pressure (and thus the relative humidity) was changed. The results support the assumption made at the start, and shows that we can detect size changes in the nanometre range with a high temporal resolution that allows us to follow the dynamics of cellular swelling.

Working with living material in the ESEM, there is a risk of dehydration. Therefore, the viability of the cells in the ESEM environment was assessed at an early stage, and the experimental procedure is described in paper II. The tests indicated a survival rate of about 95% after 90 min at 75% RH, and 60% at 50% RH. The *in situ* experiments in paper II were performed at 66%-90% RH. Viability results from previous reports vary, where some indicate a more negative impact of the ESEM environment compared to our results (Ren, Donald, & Zhang, 2008) while others show that yeast cells may survive at a relative humidity as low as 40% (Shen, 2011). The differences between the results of viability tests may stem from a number of aspects, e.g. the sample preparation and handling or the pump-down procedure used.

The acceleration voltage used when imaging the cells with the electron beam was 5 kV, and the beam was blanked whenever imaging was not needed in order to minimise the exposure. No signs of radiation damage were observed. The conditions were similar to those used in (Goponenko, 2011), where yeast cells were imaged at 5kV and at 90% RH without noticable specimen degradation.

6.2.1 Applicability to water transport activity of yeast

When studying the osmotic response of yeast cells in the ESEM, it is important to keep in mind the implications of the sample chamber environment. The response of yeast cells to osmotic chock is usually studied in aqueous media, where hyposmotic or hyperosmotic shocks can be induced by changing the osmolality of the medium. In the ESEM, by contrast, we have an environment where water vapour pressure and sample temperature are used to control the relative humidity at the specimen site. To attain high relative humidities at pressures low enough to permit imaging with sufficient quality of images, a low temperature (1°C) and water vapour pressures of 3.5-4.8 torr are used. Similar conditions have been employed in many studies where yeast cells are investigated *in situ* in the ESEM, see e.g. (Ahmad, Nakajima, Kojima, Homma, & Fukuda, 2011). However, to the author's knowledge, no study of the response to osmotic shock has previously been performed in the ESEM. It is possible that the absence of a fluid external medium in the ESEM affects the volume regulatory mechanism of cells. The export of solutes into the surrounding medium is part of the strategy of the cell in coping with osmotic swelling, and this ability may be lost in a gaseous environment.

However, the mechanisms of solute transport are not the focus of the present study, nor the target of the method development. Our focus lies rather on the

immediate effects of cell swelling and how it is affected by the presence and activity of water channels in the cell membrane. The strong cell wall of yeasts encloses the plasma membrane (Schaber, o.a., 2010) and thereby the proteins embedded in it. It is therefore reasonable to assume that the aquaporins in the yeast plasma membrane retain their structure and function in the gaseous environment of the ESEM. As a result, the *in situ* ESEM-AFM method is promising for the study of pressure-induced regulation of aquaporin channels (see section 2.2.1), a mechanism suggested by (Soveral, Madeira, Loureiro-Dias, & Moura, 2008) and (Fischer, et al., 2009) as mentioned in section 2.2.2. To the author's knowledge, no method is available at present for this type of investigation. The ability to characterise individual cells with a high sensitivity to size changes also makes it highly interesting as a complementary tool for screening of drugs directed toward the water transport activity of cells.

The next steps toward successful implementation of the technique would be to repeat the osmotic response experiments with a cantilever of lower spring constant to avoid indentation effects, and to continue the investigation beyond the wild type strain by using engineered strains with differing water transport properties. An important aspect is to establish a measurable and significant difference in the response between cells where the aquaporins have been deleted and cells where they have been overexpressed.

6.2.2 Force measurement

The developed ESEM-AFM system provides the advantage of a direct and continuous force transduction that enables the recording of cell size changes in the nanometre range and at the millisecond time scale. There are examples of other systems that combine AFM force probing with ESEM to study the mechanical and adhesion properties of yeast cells; see e.g. (Ahmad, Nakajima, Kojima, Homma, & Fukuda, 2008) and (Shen, 2011). However, these methods rely on image post-analysis to determine the force from the deflection of the AFM cantilever during indentation. The temporal resolution is then limited by the maximum frame rate (and scanning speed) that can be tolerated without compromising image quality, as the latter is decisive for the feasibility and accuracy of the analysis. Extracting force-deformation data by image analysis can be time-consuming (Stenson, 2010) and the image quality sometimes limits the possibilities to extract the wanted information (Ren, Donald, & Zhang, 2008). With our method, the force measurement does not rely on imaging at all, thereby circumventing these problems.

To avoid drift in the force reading obtained from our AFM sensor, the beam must be blanked during measurement and a few minutes before. Hence, simultaneous imaging and force recording is not practically possible. However, this is not expected to be a limitation for the *in situ* investigation of cell expansion, as the cell response could not be followed as accurately by imaging as by continuous force transduction. Also, note that on the short time scale associated with the recording of the force-distance curves for extraction of Young's modulus, drift is not a problem.

The combined ESEM-AFM system can also be applied to other materials and research questions than the one described here. Swelling is an important part of the interaction between water and soft materials. In addition to the great improvement in temporal resolution, the AFM sensor provides a more sensitive probe of size change than the images recorded during a swelling event in the ESEM. In the most general perspective, having a sensitive force probe in the ESEM enables (with some clever experimental design) the measurement of different mechanical forces on objects or structures down to the nanometre range, such as e.g. the contact force between two nanoparticles.

7 CONCLUSIONS AND FUTURE OUTLOOK

The applications of many soft biomaterials involve the interaction with water. An aspect of particular importance is water transport, which is highly dependent on the microstructure of the material and may occur in both liquid and gas phase. The environmental scanning electron microscope is a powerful tool when it comes to visualising the effects of hydration or dehydration on a specimen, facilitating the connection between microstructure and properties. However, there are still limitations when it comes to studying the transport of water through materials.

The aim of this work was to develop new *in situ* ESEM methods that enable the study of water transport in soft biomaterials. In accordance with this aim, we created a new experimental platform based on the use of a nanomanipulator and a solution for local cooling of a supporting surface in the ESEM. The resulting *in situ* sample stage has a flexible design that can accommodate samples of different geometry and enables different types of experiment related to water transport. Two applications were chosen to test and evaluate the new technique, and to demonstrate its possibilities.

The first application concerns the controlled wetting of individual cellulose fibres. For the first time, the transport of water by an isolated cellulose fibre was imaged. When the experiment was repeated using several different fibres, marked differences in absorption capacity were observed. We believe that the differences stem from a variation in fibre properties such as width, tortuosity and accessibility of lumen. Furthermore, we argue that the observed transport was dominated by liquid water flow in the lumen of the fibre.

The second application concerns the response of individual yeast cells to osmotic shock. The processes involved are intimately connected to water transport across the cell membrane. Yeast cells of the type *Pichia pastoris* were exposed to an increase in relative humidity analogous to a hyposmotic shock by raising the water vapour pressure in the ESEM. The resulting expansion was measured using a piezoresistive AFM sensor coupled with the *in situ* sample stage, and the time course could be followed in real time with high temporal resolution. The setup was also used to extract the Young's moduli of yeast cells in the ESEM. To optimise these different types of measurement, an AFM cantilever with an appropriate spring constant should be chosen separately for each application.

Our future work will build upon the technique developed within the frame of this thesis, taking advantage of the flexibility of the *in situ* sample stage. We have on-going studies in collaboration with the pharmaceutical industry, where we study thin polymer films intended as coatings for oral formulations. The aim is to increase the understanding of the water transport properties of the polymer film, which are highly dependent on its structure and composition. This is part of a higher goal to control the rate of drug release from tablets. Using the *in situ* sample stage, the films can be arranged in different orientations with respect to a water reservoir, yielding different types of information about the transport properties. Looking further ahead, the applications of the developed technique

could span a wide array of different systems and research problems concerned with the interaction between materials and water; for example, powders in the food industry, absorbents in personal care products and pulp and paper products.

ACKNOWLEDGEMENTS

Many people contributed to this work in different ways. I would like to express my gratitude to the following:

My supervisor Prof. Eva Olsson, for your steady guidance and inspiring enthusiasm. Thank you for devoting your time and for sharing your knowledge, pushing me forward on the road to becoming a scientist. With your great experience to lean on, I feel confident that I will some day be Dr. Anna Jansson!

My assistant supervisors Dr. Stefan Gustafsson and Prof. Anne-Marie Hermansson, for your invaluable contributions to the project all the way from ideas through results, evaluation and writing. Discussing with you always gives me new insights and perspectives!

My co-workers Docent Anke Sanz-Velasco, Docent Krister Svensson and Dr. Alexandra Nafari, for your enormous engagement in both projects. You have been absolutely essential for the realisation of the *in situ* ESEM techniques. I have really enjoyed working with you – both inside and outside the lab – and look forward to future collaborations!

Docent Kristina Hedfalk at the Department of Chemistry and Molecular Biology, the University of Gothenburg, for your involvement in the "yeast project". Thank you for your time and patience in answering all my questions about yeast cells, for supplying us with yeast samples and for believing in our work!

Södra Cell AB, for a fruitful collaboration in the "cellulose fibre project" and for supplying the fibre samples. A special thanks to Dr. Caroline Löfgren, for valuable discussions and support throughout the project.

The VINN Excellence Center SuMo Biomaterials, for the opportunity to work with such fascinating materials and research questions. Thanks to all my SuMo colleagues, for constructive discussions and for creating a stimulating research environment!

Vinnova for financial support of our work through SuMo Biomaterials.

The Carnegie Foundation and the Swedish Research Council for financial support of the "yeast project".

Nanofactory Instruments AB for collaboration in the method development and for invaluable help with the experimental equipment.

Abhilash Ram for your contribution to the "yeast project" through your M.Sc. thesis work.

Several valued discussion partners: Dr. Debbie Stokes, Daniel Phifer and Jonas Appelfeldt at FEI Company and Prof. Brad Thiel at the College of Nanoscale

Science and Engineering, University at Albany. Thank you for sharing your expertise on Environmental Scanning Electron Microscopy.

AstraZeneca R&D in Mölndal – especially Dr. Catherine Boissier, Dr. Mariagrazia Marucci and Mark Nicholas, for inspiring discussions on further applications of the *in situ* ESEM technique.

The Materials Science Area of Advance at Chalmers and SOFT Microscopy at Chalmers, for providing an inspiring research environment.

My colleagues in the Eva Olsson Group and at the Division of Materials Microstructure, as well as former colleagues from the Division of Microscopy and Microanalysis. You make work enjoyable and you never hesitate to lend a helping hand! I especially want to thank Dr. Anders Kvist, for your help with the microscopes and Ola Löfgren, for your help with computer issues. Nothing would work without you! A special thanks also to my office room mates, formerly Dr. Mattias Thuvander and presently Torben Pingel, for making life in the office more fun!

Rune Johansson, for being "en klippa" in the workshop! Thank you for all your help in crafting (and recrafting!) parts of the experimental equipment.

My beloved family: Mamma, Steffo, Jessica, Jimmy, Mormor, Berit and all the rest of you! (You are so many, I can't name you all ☺.) You have always supported and encouraged me, and for that I am deeply thankful!

My darling Robert, it's impossible to boil down to a few words how much you mean to me. Thank you for your unfailing support and love, and for your patience with me, my work and my temper! You are also my personal Microsoft Office and Photoshop expert, which I greatly appreciate. ☺

Finally, my little Vilma, thank you for being the best thing that ever happened to me!

REFERENCES

Ahmad, M. R., Nakajima, M., Kojima, S., Homma, M., & Fukuda, T. (2011). Buckling nanoneedle for characterizing single cells mechanics inside environmental SEM. *IEEE Transactions on Nanotechnology , 10* (2), 226-236.

Ahmad, M. R., Nakajima, M., Kojima, S., Homma, M., & Fukuda, T. (2008). In situ single cell mechanics characterization of yeast cells using nanoneedles inside environmental SEM. *IEEE Transactions on Nanotechnology , 7* (5), 607-616.

Ahmad, M. R., Nakajima, M., Kojima, S., Homma, M., & Fukuda, T. (2007). Mechanical properties characterization of individual yeast cells using environment-SEM nanomanipulation system. *IEEE International Conference on Intelligent Robots and Systems* , 596-601.

Ahmad, M. R., Nakajima, M., Kojima, S., Homma, M., & Fukuda, T. (2010). Nanoindentation methods to measure viscoelastic properties of single cells using sharp, flat, and buckling tips inside ESEM. *IEEE Transactions on Nanobioscience , 9* (1), 12-23.

Ahmad, M. R., Nakajima, M., Kojima, S., Homma, M., & Fukuda, T. (2008). The effects of cell sizes, environmental conditions, and growth phases on the strength of individual W303 yeast cells inside ESEM. *IEEE Transactions on Nanobioscience , 7* (3), 185-193.

Andreasson, B., Forsström, J., & Wågberg, L. (2003). The porous structure of pulp fibres with different yields and its influence on paper strength. *Cellulose , 10*, 111-123.

Bergman, R., Cai, Z., Carll, C. G., Clausen, C. A., Dietenberger, M. A., Falk, R. H., et al. (2010). *Wood handbook - Wood as an engineering material.* U.S. Department of Agriculture, Forest Service, Forest Products Laboratory. Madison, WI: Forest Products Laboratory.

Camacho-Bragado, G. A., Dixon, F., & Colonna, A. (2011). Characterization of the response to moisture of talc and perlite in the environmental scanning electron microscope. *Micron , 42* (3), 257-262.

Côté, W. A. (1967). *Wood Ultrastructure.* Seattle: University of Washington Press. Donald, A. M., He, C., Royall, C. P., Sferrazza, M., Stelmashenko, N. A., & Thiel, B. L. (2000). Applications of environmental scanning electron microscopy to colloidal aggregation and film formation. *Colloids and Surfaces A: Physicochemical and Engineering Aspects , 174* (1-2), 37-53.

Dragnevski, K. I., & Donald, A. M. (2008). An environmental scanning electron microscopy examination of the film formation mechanism of novel acrylic latex. *Colloids and Surfaces A: Physicochemical and Engineering Aspects , 317* (1-3), 551-556.

Dufek, M., & Hayles, M. (2003). The Quanta FEG 200, 400, 600 User's Operation Manual. *First edition*. FEI Company.

Fernandes Diniz, J. M., Gil, M. H., & Castro, J. A. (2004). Hornification - Its origin and interpretation in wood pulps. *Wood Science and Technology , 37* (6), 489-494.

Fischer, G., Kosinska-Eriksson, U., Aponte-Santamaría, C., Palmgren, M., Geijer, C., Hedfalk, K., et al. (2009). Crystal structure of a yeast aquaporin at 1.15 angstrom reveals a novel gating mechanism. *Public Library of Science Biology , 7* (6).

Gellerstedt, F., Wågberg, L., & Gatenholm, P. (2000). Swelling behaviour of succinylated fibers. *Cellulose , 7* (1), 67-86.

Gennemark, P. (2005). *Modeling and identification of biological systems with emphasis on osmoregulation in yeast.* Chalmers University of Technology, Department of Computer Science and Engineering. Gothenburg: Chalmers University of Technology.

Goponenko, A. V., Boyle, B. J., Jahan, K. I., Gerashchenko, M. V., Fomenko, D. E., Gladyshev, V. N., et al. (2011). Use of environmental scanning electron microscopy for in situ observation of interaction of cells with micro- and nanoprobes. *Micro and Nano Letters , 6* (8), 603-608.

Hedfalk, K., Törnroth-Horsefield, S., Nyblom, M., Johanson, U., Kjellbom, P., & Neutze, R. (2006). Aquaporin gating. *Current Opinion in Structural Biology , 16* (4), 447-456.

Jenkins, L. M., & Donald, A. M. (1999). Contact angle measurements on fibers in the environmental scanning electron microscope. *Langmuir , 15* (22), 7829-7835.
Jenkins, L. M., & Donald, A. M. (2000). Observing fibers swelling in water with an environmental scanning electron microscope. *Textile Research Journal , 70* (3), 269-276.

Jenkins, L. M., & Donald, A. M. (1997). Use of the environmental scanning electron microscope for the observation of the swelling behaviour of cellulosic fibres. *Scanning , 19* (2), 92-97.

Köhnke, T., Lund, K., Brelid, H., & Westman, G. (2010). Kraft pulp hornification: A closer look at the preventive effect gained by glucuronoxylan adsorption. *Carbohydrate Polymers , 81* (2), 226-233.

Karlsson, J. O., Andersson, M., Berntsson, P., Chihani, T., & Gatenholm, P. (1998). Swelling behavior of stimuli-responsive cellulose fibers. *Polymer , 39* (16), 3589-3595.

King, L. S., Kozono, D., & Agre, P. (2004). From structure to disease: The evolving tale of aquaporin biology. *Nature Reviews Molecular Cell Biology , 5* (9), 687-698.

Klipp, E. N. (2005). Integrative model of the response of yeast to osmotic shock. *Nature Biotechnology , 23* (8), 975-982.

Laivins, G., & Scallan, V. (1993). The mechanism of hornification of wood pulps. In C. Baker (Ed.), *Products of papermaking* (pp. 1235-1260). Oxford: Pirs International.

Lanero, T., Cavalleri, O., Krol, S., Rolandi, R., & Gliozzi, A. (2006). Mechanical properties of single living cells encapsulated in polyelectrolyte matrixes. *Journal of Biotechnology , 124* (4), 723-731.

Marechal, P., Martinez de Marafion, I., Molin, P., & Gervais, P. (1995). Yeast cell responses to water potential variations. *International Journal of Food Microbiology , 28* (2), 277-287.

Marmarou, A. (2004). The pathophysiology of brain edema and elevated intracranial pressure. *Cleveland Clinic journal of medicine , 71 Suppl 1*, S6-8.

Montes-H, G., Geraud, Y., Duplay, J., & Reuschle, T. (2005). ESEM observations of compacted bentonite submitted to hydration/dehydration conditions. *Colloids and Surfaces A (Physicochemical and Engineering Aspects) , 262* (1-3), 14-22.

Nafari, A. (2010). *Microsensors for In Situ Electron Microscopy Applications.* Gothenburg: Doktorsavhandlingar vid Chalmers tekniska högskola.

Nafari, A., Karlen, D., Rusu, C., Svensson, K., Olin, H., & Enoksson, P. (2008). MEMS sensor for in situ TEM atomic force microscopy. *Journal of MicroElectroMechanical Systems , 17* (2), 328-333.

Pasantes-Morales, H., & Cruz-Rangel, S. (2010). Brain volume regulation: Osmolytes and aquaporin perspectives. *Neuroscience , 168* (4), 871-884.

Perkins, E. L., & Batchelor, W. J. (2012). Water interaction in paper cellulose fibres as investigated by NMR pulsed field gradient. *Carbohydrate Polymers , 87* (1), 361-367.

Reingruber, H., Zankel, A., Mayrhofer, C., & Poelt, P. (2012). A new in situ method for the characterization of membranes in a wet state in the environmental scanning electron microscope. *Journal of Membrane Science , 399-400*, 86-94.

Ren, Y., Donald, A. M., & Zhang, Z. (2008). Investigation of the morphology, viability and mechanical properties of yeast cells in environmental SEM. *Scanning , 30* (6), 435-442.

Rizzieri, R., Baker, F. S., & Donald, A. M. (2003). A tensometer to study strain deformation and failure behavior of hydrated systems via in situ environmental

scanning electron microscopy. *Review of Scientific Instruments , 74* (10), 4423-4428.

Rowell, R. (2012). Handbook of Wood Chemistry and Wood Composites, Second Edition. CRC Press.

Schaber, J., Adrover, M. Á., Eriksson, E., Pelet, S., Petelenz-Kurdziel, E., Klein, D., et al. (2010). Biophysical properties of Saccharomyces cerevisiae and their relationship with HOG pathway activation. *European Biophysics Journal , 39* (11), 1547-1556.

Shen, Y., Nakajima, M. R., Ahmad, M., Kojima, S., Homma, M., & Fukuda, T. (2011). Effect of ambient humidity on the strength of the adhesion force of single yeast cell inside environmental-SEM. *Ultramicroscopy , 111* (8), 1176-1183.

Sjöström, E. (1993). *Wood Chemistry - Fundamentals and Applications* (Second ed.). San Diego, CA, USA: Academic Press.

Smith, A. E., Zhang, Z., Thomas, C. R., Moxham, K. E., & Middelberg, A. P. (2000). The mechanical properties of Saccharomyces cerevisiae. *Proceedings of the National Academy of Sciences of the United States of America , 97* (18), 9871-9874.

Somero, G., & Yancey, P. (1997). In J. J. Hoffman (Ed.), *Handbook of Physiology* (pp. 441-484). Oxford: Oxford University Press.

Soveral, G., Madeira, A., Loureiro-Dias, M. C., & Moura, T. F. (2008). Membrane tension regulates water transport in yeast. *Biochimica et Biophysica Acta - Biomembranes , 1778* (11), 2573-2579.

Stenson, J. D., Hartley, P., Wang, C., & Thomas, C. R. (2011). Determining the mechanical properties of yeast cell walls. *Biotechnology Progress , 27* (2), 505-512.

Stenson, J. D., Ren, Y., Donald, A. M., & Zhang, Z. (2010). Compression testing by nanomanipulation in environmental scanning electron microscope. *Experimental Techniques , 34* (2), 60-62.

Stokes, D. J. (2008). *Principles and Practice of Variable Pressure/ Environmental Scanning Electron Microscopy (VP-ESEM).* West Sussex, UK: John Wiley & Sons Ltd.

Svensson, K., Jompol, Y., Olin, H., & Olsson, E. (2003). Compact design of a transmission electron microscope-scanning tunneling microscope holder with three-dimensional coarse motion. *Review of Scientific Instruments , 74* (11), 4945-4947.

Tamás, M. J., Karlgren, S., Bill, R. M., Hedfalk, K., Allegri, L., Ferreira, M., et al. (2003). A short regulatory domain restricts glycerol transport through yeast Fps1p. *Journal of Biological Chemistry , 278* (8), 6337-6345.

Theliander, H., Paulsson, M., & Brelid, H. (2002). *Introduktion till massa- och pappersframställning.* Göteborg: Chalmers tekniska högskola.

Thiel, B. L., & Donald, A. M. (1992). In situ mechanical testing of fully hydrated carrots (daucus carotd) in the environmental SEM. *Annals of Botany , 82* (6), 727-733.

Wei, Q., Mather, R. R., Fotheringham, A. F., & Yang, R. D. (2002). Observation of wetting behavior of polypropylene microfibers by environmental scanning electron microscope. *Journal of Aerosol Science , 33* (11), 1589-1593.

Weisenhorn, A. L., Khorsandi, M., Kasas, S., Gotzos, V., & Butt, H. J. (1993). Deformation and height anomaly of soft surfaces studied with an AFM. *Nanotechnology , 4* (2), 106-113.

Verbalis, J. G. (2010). Brain volume regulation in response to changes in osmolality. *Neuroscience , 168* (4), 862-870.

Öberg, F., & Hedfalk, K. (2012). Recombinant production of the human aquaporins in the yeast Pichia pastoris. *Molecular Membrane Biology , Early Online*, 1-17.

Östlund, Å., Köhnke, T., Nordstierna, L., & Nydén, M. (2009). NMR cryoporometry to study the fiber wall structure and the effect of drying. *Cellulose , 17* (2), 321-328.